NASA CONTRACTOR REPORT

NASA CR-61

NASA CR-61

AN INFRARED INTERFERENCE SPECTROMETER — ITS EVALUATION, TEST, AND CALIBRATION

by Lucien W. Chaney and Leslie T. Loh

Prepared under Contract No. NASr-54 (03) *by*
UNIVERSITY OF MICHIGAN
Ann Arbor, Michigan
for

NATIONAL AERONAUTICS AND SPACE ADMINISTRATION • WASHINGTON, D. C. • JUNE 1964

AN INFRARED INTERFERENCE SPECTROMETER - ITS EVALUATION, TEST, AND CALIBRATION

By Lucien W. Chaney and Leslie T. Loh

Prepared under Contract No. NASr-54(03) by
UNIVERSITY OF MICHIGAN
Ann Arbor, Michigan

NATIONAL AERONAUTICS AND SPACE ADMINISTRATION

For sale by the Office of Technical Services, Department of Commerce
Washington, D.C. 20230 -- Price $1.50

TABLE OF CONTENTS

TABLE OF CONTENTS (Concluded)

LIST OF FIGURES

1. INTRODUCTION

The Meteorological Satellite Branch of Goddard Space Flight Center, National Aeronautics and Space Administration, has been supporting an investigation by The University of Michigan High Altitude Engineering Laboratory into the possibilities of adapting Fourier transform spectroscopy (using a Michelson interferometer) to measurement of the earth's thermal radiation. The interferometric technique has been described by Strong,[1,2] Gebbie,[3] and Felgett.[4]

Previous applications of the technique have included measurements in the far-infrared, measurements of night glow, and high resolution studies where the available signals are too low for conventional spectroscopy. The principal advantage of the technique over conventional spectroscopy is its increased signal-gathering power. In a theoretically perfect instrument, power can be increased in two ways:

1) All the wavelengths are observed simultaneously rather than one resolution element at a time. This results in an increase in signal-to-noise ratio equal to $\sqrt{N}/2$, where N is the number of resolution elements. The factor of 1/2 results from the fact that on the average, one-half the energy is reflected away from the instrument.

2) For any given resolution ratio, energy can be accepted from a much larger solid angle. The instrumental line shape of a conventional spectrometer has the form $(\sin y/y)^2$, whereas the interferometer line shape is $\sin y/y$ where y is the lateral distance across the instrument aperture.

In addition to these fundamental advantages there is an engineering advantage in that for the same light-gathering power the instrument can be made physically smaller.

The principal disadvantage of the technique is that the final results are not obtained directly: It is necessary to make a Fourier transform of the output signal to obtain spectrographic information. High-speed digital computers such as the IBM 7090 offer a practical means of accomplishing this result.

In the initial phase of our investigation of the technique, we became aware that Block Associates was manufacturing an instrument which might meet our requirements.

Our original specifications called for a spectral range of 4-30μ, reso-

lution of 10 cm^{-1}, and a 5-sec scan time. The Block I-4 interferometer has the following specifications: spectral range 2-15μ, resolution 40 cm^{-1}, and scan time 1 sec. These were sufficiently close to the original specifications to warrant the purchase of an I-4 unit in lieu of developing one of our own.

The Block instrument represents a significant departure from previous instruments in that a Fourier series analysis of the output signal can be made. This is accomplished with a wave analyzer, eliminating the need for a high-speed computer.

Details of the work in evaluating, testing, and calibrating the Block instrument are given below.

2. DESCRIPTION OF THE INSTRUMENT

The Block I-4 interferometer, in common with all interferometers used for Fourier transform spectroscopy, is a Michelson type. The novel feature of the Block design (Fig. 1) is the method of driving the mirror. The driver is a coil, spring mounted, in a magnetic field. The parallel springs restrain the mirror motion to a single plane and direction. A linear sawtooth of voltage is applied to the drive coil, which moves the mirror linearly provided a constant spring rate is maintained.

2.1. THEORY

The basic operation is as follows: The incoming radiation I_o is split by the beam splitter and recombined so that an average energy $I_o/2$ is directed toward the detector.

When the instrument is properly adjusted with nearly monochromatic light, circular fringes can be observed at the output. The central fringe is focused on the detector so that variations in the intensity of this fringe will produce a corresponding variation in output signal. The bolometer output, when plotted vs mirror position, is called an interferogram (Fig. 2). The Fourier transform of the interferogram is the spectrogram of the input radiation.

If the input radiation is monochromatic, then the radiation falling on the detector will be

$$I(x) = \frac{I(\nu)}{2} [1 + \cos 2\pi\nu x] \qquad (1)$$

where

$I(\nu)$ = the input radiation times the spectral response of the instrument.

x = the difference in path length between beams

ν = the wave number of the input radiation

For heterochromatic radiation, the general expression becomes

$$I(x) = \int_{-\infty}^{\infty} \frac{I(\nu)}{2} [1 + \cos 2\pi\nu x] d\nu \qquad (2)$$

2.1.1. Fourier Transform Theory

In the case of the I-4 interferometer the limits of integration are more specific:

$$I(x) = \int_{560\ cm^{-1}}^{5000\ cm^{-1}} \frac{I(\nu)}{2} [1 + \cos 2\nu x] d\nu \qquad (3)$$

When $x = 0$,

$$I(o) = \int_{560\ cm^{-1}}^{5000\ cm^{-1}} I(\nu)\, d\nu \qquad (4)$$

When $x = \infty$,

$$I(\infty) = \int_{560\ cm^{-1}}^{5000\ cm^{-1}} \frac{I(\nu)}{2}\, d\nu = \frac{Io}{2} \qquad (5)$$

If the d-c component $I(o)/2$ is subtracted from $I(x)$, the remainder is the interferogram function.

$$F(x) = \int_{560\ cm^{-1}}^{5000\ cm^{-1}} I(\nu)/2 \cos 2\pi\nu x d\nu \quad \text{(See Fig. 2)} \qquad (6)$$

$I(\nu)$ can be determined by the Fourier theorem:

$$I(\nu) = 2\int_{-\infty}^{\infty} F(x) \cos 2\pi\nu x dx \qquad (7)$$

However, in our case the integral extends not from $-\infty$ to $+\infty$ but from $-B/2$ to $B/2$, where B is the total path displacement. Therefore,

$$I(\nu) = 2\int_{-B/2}^{+B/2} F(x) \cos 2\pi\nu x dx \qquad (8)$$

But this can be true only if $F(B/2)$, $F(-B/2)$, and all subsequent values are equal to zero. This is, of course, one of our basic assumptions.

In the case of the I-4, distance is not measured directly; rather amplitude is recorded as a function of time. Referring to Fig. 3, we can write

$$x = (B/T)t \tag{9}$$

where

x = optical displacement (cm)

B = maximum displacement (cm)

T = linear sweep time (sec)

t = instantaneous value of time

If we substitute (9) into (6) and rewrite (8), then

$$I(\nu) = 2 \int_0^T F(t) \cos 2\pi\nu \frac{B}{T} t \, dt \tag{10}$$

provided F(o) and F(T) are equal to zero.

This is the equation which is used to solve for values of $I(\nu)$. The interferogram is plotted by a recording oscillograph (C.E.C.)* at a paper speed of 64 in./sec (see Fig. 8). The values of F(t) are measured with the aid of a Benson-Lehner chart reader coupled to an IBM card punch. Using the values thus tabulated, a numerical solution of Eq. (10) is obtained for each of the desired values of $I(\nu)$ on the 7090 computer.

2.1.2. Fourier Series Theory

Referring to Eq. (10), we can see that there is a definite frequency $f = \nu B/T$ associated with each wave number ν. The amplitude of this frequency component corresponds to the value of $I(\nu)$. This value could be measured with the proper analog computer, but a standard wave analyzer can not make the measurement due to its long time constant.

An alternate approach to this problem is to make the interferogram a repetitive function with a period of T' and to measure the amplitudes of the harmonics which are generated.

The amplitude of the repetitive interferogram function (Fig. 4) in the period from 0 to T is given by the expression

$$F(t) = \int_{560\ cm^{-1}}^{5000\ cm^{-1}} \frac{I(\nu)}{2} \cos 2\pi\nu \frac{B}{T} t \, d\nu \tag{11}$$

*Consolidated Electrodynamics Corporation—Recording Oscillograph Model 5-124.

which is derived by substituting (9) into (8). This function can also be expressed as a Fourier Series:

$$F(t) = \frac{a_0}{2} + \sum_{n=1}^{\infty} \left[a_n \cos \frac{2\pi nt}{T'} + b_n \sin \frac{2\pi nt}{T'} \right] \tag{12}$$

Then by Fourier's Theorem

$$a_n = E(n) = \frac{2}{T'} \int_0^{T'} F(t) \cos \frac{2\pi nt}{T'} \, dt \tag{13}$$

The frequency associated with this function is $f' = n/T'$.

If we compare Eq. (10) with Eq. (13) it can be seen that when $T = T'$ and $n = \nu B$, the equations are identical. The difference between T and T' will make a scale factor change only if F(t) is equal to zero in the interval from T to T'. However, $n = \nu B$ for discrete values of ν only, since n is an integral number whereas ν can have any value.

The associated frequency f can have any value within the limits corresponding to values of ν from 560-5000 cm^{-1}. However, f' can only have discrete values separated by $\Delta f'$, where $\Delta f' = 1/T$.

Hence,

$$I(\nu) \rightarrow E(n)'$$

as

$$\Delta f' \rightarrow 0$$

and as

$$T' \rightarrow \infty$$

How large T' must be in a practical case depends on the shape of the original function. The general conclusion based on our experimental results is that if $T' = 2T$ there will be no measurable difference between $I(\nu)$ and E(n).

2.2. PHYSICAL DESCRIPTION

2.2.1. Optics

The entire optics of the I-4 is built around an approximately 2-1/2-in. cube (Fig. 5). The optics are packaged inside a 7-1/2 x 6-1/2 x 3-1/2-in. cast frame. This is known as the head and contains, in addition to the optics, the preamplifier and the DC to DC converter. The converter is required to generate the detector bias voltage and the preamplifier supply voltage.

2.2.2. Main Amplifier

The basic parts of the interferometer are shown in Fig. 6, an assembly drawing of the flight package.

Mounted next to the head in the center of the package is the main amplifier. This unit is 5-3/4 x 7-1/2 x 6-3/4-in. and contains two voltage regulators for both the negative and the positive power supplies, a sweep generator and amplifier unit which produces the linear sweep voltage, and a 250X amplifier.

2.2.3. Battery Pack

The battery pack is 6-1/2 x 3-7/8 x 6-1/4-in. and contains three separate supplies: one 40-volt (1000 milliampere-hours) and two 20-volt (14,000 milliampere-hours). The 40-volt pack supplies the 250X signal amplifier. One of the 20-volt packs supplies the negative regulator and the other supplies the positive regulator.

2.2.4. R-F Filters

Mounted in a long narrow box along the rear edge of the package are the r-f filters. Every lead which comes into the package passes through an r-f filter. In the early phase of the work, interference and cross talk, were obtained when the interferometer was mounted near the telemetry. However, by placing the entire unit inside the copper shield can and using r-f filters on every lead this problem was completely eliminated.

2.2.5. Blackbody

In Fig. (6) the flight blackbody drive is shown attached to the right

side of the head. It consists of a magnesium shutter 2 x 2-1/2 x 1/8 in. into which v-shaped grooves have been ruled. These grooves have an angle of 30° and are .075 deep. The radius on the tips and in the valleys is less than .001 in. The blackbody is normally left in the retracted position, in which the underside is exposed to space through a periscope mounted under the package. We are hoping that by this technique a temperature differential of at least 10° can be maintained between the blackbody and the head. Once every 15 min the blackbody is driven to the calibrate position in front of the optics. It stays there for a period of 50 sec.

2.2.6. Voltage and Temperature Monitors

Placement of the flight timer external to the interferometer permits the monitoring of voltages and temperatures at 5-min intervals during the flight. The voltages monitored are the three power supplies and the output of one voltage regulator. The temperatures monitored are the bolometer, the cube aperture, the blackbody, and the case.

The thermistors on the bolometer, aperture, and blackbody are YSI* precision thermistors. The combination of precision thermistors, precision resistors, and regulated supply makes it possible to measure temperatures to 0.2°C. The bolometer thermistor is mounted directly under the bolometer on the copper block.

2.2.7. Temperature Control

The bolometer mount (Fig. 5) was redesigned to include heaters and a thermostat. The heaters are eight standard 1/2-watt resistors wired in a series-parallel combination. These were imbedded into the mount so that the source of heat would be as close to the bolometer as possible. The thermostat which controls the heating is also imbedded in the mount. The thermostat controls the temperature to ±0.2°C over short periods, but over long periods it tends to drift approximately 1.5°C.

*Yellow Spring Instrument Co.—Precision Thermistor Model No. 44006.

3. DATA REDUCTION

As indicated in the description, two separate methods of data reduction have been investigated. The first method, which has been used by all previous workers in this field, is to solve numerically for the Fourier transform of the interferogram. The second method is to make a repetitive function of a series of interferograms, obtaining the Fourier coefficients by use of a wave analyzer.

3.1. FOURIER TRANSFORM ANALYSIS

The data reduction procedure is outlined in Fig. 7. The interferometer output signal is fed through the VCO transmitter-antenna-receiver and stored on magnetic tape. The tape recorder is equipped with tapespeed compensation to compensate for any "wow and flutter" effects. The signals are then played back through the discriminator and the output is displayed on a direct writing oscillograph.

The gain of the oscilloscope is set so that a maximum signal will produce approximately a 6-in. deflection. A sawtooth signal from a precision oscillator (H-P Model No. 302A) is fed to another channel of the oscillograph. This signal is set on the extreme edge of the chart with an amplitude equal to 1/2 in. and a frequency which corresponds to 1μ in path difference. When an interferogram is to be recorded, the paper is driven at 64 cps. Thus, a single interferogram is recorded on an 8-in. strip approximately 30 in. long (Fig. 8). A zero reference line is drawn through the end points of the oscillogram and the mirror zero line is drawn through the amplitude maximum. These lines are used as reference in setting the chart on the Benson-Lehner chart reader. The 1-μ marker signal and the peak of the interferogram are phased together. The amplitude is read at each 1-μ interval and this information is automatically processed by the IBM punch.

The final results are obtained from the 7090 computer. The computer program performs the following functions:

1) Computes the value of the transform at a set of given wave numbers.

2) Searches a calibration table and interpolates for the corresponding value of temperature.

3) Applies a correction factor corresponding to bolometer temperature.

4) Plots temperature vs wave number.

Considering the equipment available to us, this method of data reduction has several disadvantages:

1) The elapsed time from the receipt of the data to the final results is at least one day. This is satisfactory for final flight data but not for experimental procedures.

2) The operational time required to process each inteferogram is approximately 2 hr. Most of this time is spent measuring the interferogram ordinates and punching the IBM cards.

3) The final results are relatively noisy since the data processed is a single interferogram.

An advantage of this method is that it precludes uncertainty as to the real value of the transform.

3.2. WAVE ANALYZER OR FOURIER SERIES ANALYSIS

This method of data reduction is outlined in Fig. 9. The line which includes the interferometer through the magnetic tape recorder is identical to the corresponding line in Fig. 7.

The data to be reduced is transcribed to the loop tape recorder (Fig. 10). This is an Ampex Series 300* tape recorder which has been modified for loop operation. The loop length is cut so that it corresponds as closely as possible to exactly 35 interferograms. The signal is recorded on an FM channel at 7.5 in./sec. The recording is always done such that the end overlaps the start. This is possible in FM recording since the new information completely erases the previous recording.

The playback is performed at 60 cps, producing an 8-to-1 frequency multiplication. The output signal is analysed with a H-P Model 302A wave analyzer. The bandwidth of the wave analyzer is 8 cps and the spacing between harmonics is 14 cps; hence, each coefficient is measured separately.

The wave analyzer output is recorded on an x-y plotter. The analyzer drive provides an x output which is proportional to frequency. Hence, the plot is harmonic amplitude vs wave number. The amplitude of each harmonic corresponds to a given temperature as determined by a previous blackbody calibration. This information is stored as two third-order equations in the LPG-30. Each equation corresponds to the maximum and minimum bolometer temperature. The coefficients of the equation to be used for a given bolometer temperature are determined by interpolation.

An operator is required to read the amplitude of each harmonic and its corresponding wave number into the LPG-30 program. The final results, equiv-

*Ampex Corporation—Model S-3657 magnetic tape recorder.

alent blackbody temperature vs wave number, are plotted by a Cal-Comp* plotter attached to the output of the LPG-30.

This system has several advantages:

1) The elapsed time between recording the data and the transform is less than 10 min.

2) The complete data reduction requires approximately 1/2 hr per interferogram.

3) The integration of 35 interferograms reduces the system noise.

The disadvantages are:

1) The uncertainty as to how closely the amplitude of the harmonics corresponds to the transform.

2) A periodic noise signal is introduced by the loop recorder. This is due to the stopping transient which occurs at the end of the recording.

*California Computer Products, Inc.--Model 560R Digital Incremental Recorder.

4. CALIBRATION OF INSTRUMENT

4.1. WAVELENGTH CALIBRATION

The wavelength calibrations were made by three methods: (1) viewing a quartz infrared lamp through a set of interference filters, (2) using the 13-U Perkin-Elmer spectrometer as a monochromator, and (3) using point-to-point comparison with a calibrated spectra of polystyrene (Fig. 11).

The initial calibrations were made by methods (1) and (2). There was very good agreement between the two methods, and the discrepancy between different interference filters was thought to be within the experimental errors.

Since the I-4 can be operated at various mirror-sweep lengths and rates, wavelength calibrations were made under all conditions. This data (Fig. 12) shows good agreement between different calibrating wavelengths and the interdependence of sweep length and rate. The values shown in Fig. 12 are the equivalent length for the total period and are longer than the true distance. After using the instrument for some time, a single sweep length and rate were selected. The nominal length is 250μ and the period is 0.5 sec. These values were chosen so that all of the frequency components would be within the pass band of the instrument, and the harmonics could be individually resolved.

The final calibration was performed by measuring the wavelengths of the transmission maxima of a sample of polystyrene on a Perkin-Elmer 13-U spectrometer. This sample was then used as a standard for calibrating the interferometer. It was thus possible to derive a calibration curve for the instrument (Fig. 13).

4.2. AMPLITUDE CALIBRATION

Amplitude calibrations have been attempted by several methods, as described below.

4.2.1. Quartz Lamps

Calibration curves on quartz lamps were available from the manufacturer. Our attempts to use these units proved to be very unsatisfactory, largely because our original interferometer peaked at 12μ whereas the quartz lamp peaked at 1μ. The quartz tube is heated by the shorter wavelengths and reradiates as a larger-diameter blackbody in the 12-μ region; therefore the

radiation curves supplied by the manufacturer are not valid.

4.2.2. Infrared Lamps and Filters

The idea in this case was to make ratio measurements by inserting filters with known spectral transmission. This proved to be impossible for two reasons: (1) the filters tend to reradiate at a longer wavelength; and (2) small wavelength errors can cause large amplitude errors.

4.2.3. High-Temperature Blackbody

A conical blackbody which fit into a ceramic cone heater was constructed. It operated at a nominal temperature of 500°C, but there was a temperature gradient of 80°C from the aperture to the apex. Therefore it was abandoned, and a "frying pan" blackbody, which can operate at 200°C, was used for calibration in the 7-3μ range.

4.2.4. Low-Temperature Blackbody (-78°C to +25°C)

Since this device (Fig. 14) most closely simulates the earth's thermal radiation, it has been used for the majority of our calibrations.

The blackbody is a 15° cone, with an approximately 2-1/2 in. opening, welded into a 1-cu-ft aluminum box. The box is covered on all sides by 2 in. of styrofoam. Mounted in the box is a 1200-watt immersion heater used to raise the temperature. A diaphragm shutter is mounted on the blackbody opening inside the dry box.

The operation is as follows: The interferometer is placed inside the dry box and adjusted so that the target fills the field of view. A dish of phosphorus pentoxide is placed inside and left covered. All the openings are closed and sealed with masking type. The box is then flushed with nitrogen and the phosphorus pentoxide is uncovered. The target container is filled with ethyl alcohol and dry ice is slowly added. Approximately 45 min is required to lower the temperature to -78°C.

The evaporating CO_2 tends to stir the alcohol, but prior to recording each data point, vigorous stirring is required to obtain a temperature differential of less than 0.5°C along the cone. The cone temperature is monitored by five thermocouples imbedded along its length.

The bolometer temperature is maintained at a constant temperature of ±0.2°C by adjusting the heater supply voltage.

The recording of data follows the procedure described in Section 3.2. A calibration sequence is started at -78°C, and data is usually taken at 10°C-intervals covering the temperature range.

Without the application of heat, the cone temperature will change 1°C in 15 min at -70°C. The heater can raise the temperature 10°C in 4 min.

4.2.5. Vacuum Calibrator[8] (+50°C to -190°C)

This calibrator was designed specifically for the TIROS 5-channel radiometer calibrations and has not yet been adapted to interferometer calibrations. We plan to use this equipment in the future in order to make calibrations below -78°C, which are required for making sky measurements.

5. SOURCES OF ERROR

5.1. SPECTRAL RESPONSE

The overall spectral response of the instrument is given in Fig. 15. This curve was derived by assuming an ideal blackbody distribution for our calibration devices. The spectral response represents deviations from this curve.

The factors which lead to deviations are described below.

5.1.1. Window

The present window is made of NaCl, and its transmissivity[5] decreases rapidly for wavelengths beyond 15μ. A KRS-5 window, which was also supplied with the instrument, could be used to extend the long-wavelength transmission, at a sacrifice of signal inside the pass band.

5.1.2. Beam Splitter and Compensating Plate

The beam splitter and compensating plate are made from NaCl and the semi-transparent coating is germanium. The radiation makes a total of four passages through these two layers, which further reduces the signal beyond 15μ.

The germanium[5] has a very sharp cutoff near 2μ on the short-wavelength side and a gradual cutoff beyond 15μ on the long-wavelength side.

5.1.3. Mirrors

The mirrors are $\lambda/4$ front surface aluminum. A typical spectrum[6] of a mirror of this type indicates that the reflectivity is relatively constant at 91% from 4-14μ. The reflectivity drops to 78% at 16μ, and to 86% at 8.5μ. This variation will directly affect the response of the instrument.

5.1.4. Lenses

Two KRS-5 lenses are used in the interferometer. This material is transparent in the region from 2-16μ.[5] However, for two surfaces there is a reflection loss of 28.4% which applies equally to all wavelengths. The total loss for two lenses is 49%.

5.1.5. Bolometer

The bolometer itself has a reflectivity which varies as a function of wavelength. The paint "Zapon" used on the detector has several dips in the region of interest. We could explain an observed dip of 20% in the response of the instrument at 11μ only as a function of the detector. Recent data from Barnes Engineering[7] indicates that this dip can be explained by the reflectivity of the Zapon paint used on the thermistor.

5.1.6 Light Path Divergence

The interferometer accepts energy from a solid angle of 14°. Hence, the path of the energy which travels along the outside ray is longer than that of the energy which travels along the axis. Referring to Fig. 16, the most divergent ray, 1, enters the interferometer at an angle γ, moves past the aperture and strikes the semi-transparent mirror M_1. Ray 1 divides, one-half being reflected as ray 2 and one-half being transmitted as ray 3. Ray 3 is reflected from M_2 as ray 4. The difference in path length between rays 2 and 4 is $2B + \lambda_m$. The difference in path length along the centerline is 2B. Let B be the maximum excursion of the movable mirrors; then λ_m equals the minimum wavelength modulated by the interferometer.

Now:

$$\lambda_m \cong 2\gamma^2 B$$

and with

$$\gamma = .122, \quad B = 125\mu$$

we have

$$\lambda_m = (.122)^2 \times 2 \times 125 = 3.75\mu$$

Hence, all wavelengths shorter than 3.75μ will not be modulated by path lengths in excess of 250μ. This fact sets the resolution limit of the instrument.

5.2. MIRROR MOTION

We have generally assumed that the motion of the movable mirror is perfectly parallel and linear with time. We will now consider deviations from this ideal situation.

5.2.1. Deviation from Parallel

By deviations from parallel we mean that as the mirror travels in a direction x, it tends to move through an angle θ (Fig. 17). This will displace the optical axis of the instrument so that less energy falls on the detector. The effect on the interferogram is to make the signal nonsymmetric. This situation is depicted in Fig. 18 which compares the ideal with the non-symmetric interferogram. In the nonsymmetric case, the sensitivity is greater on the left side than on the right (Fig. 19)

5.2.2. Nonlinear Motion

The idealized mirror motion as a function of time is plotted in Fig. 3. If the motion were perfect there would be a constant 1-to-1 relation between the input radiation and the electrical frequencies generated. The wavelength calibration curve (Fig. 13) indicates the degree of nonlinearity. This data shows that the electrical frequencies must be multiplied by a larger constant for the shorter wavelengths (indicating a slower motion in the central portion of the travel).

5.3. TEMPERATURE EFFECTS

5.3.1. Detector

Any change in the ambient temperature tends to change the detector temperature, which in turn changes the output. Without additional heating, the detector requires 4 hr to reach a stable temperature (Fig. 20). However, a change in ambient or target temperature will cause the detector to deviate. At first we tried to calibrate the instrument over a range of detector temperatures (24°C to 32°C), but this proved to be difficult due to the "pulling" of the detector temperature by the target.

Our solution to this problem has been to install an electric heater and thermostat in the bolometer mount. The variations, ±1.5°C, are much smaller than those previously encountered. Although it is still necessary to calibrate at different bolometer temperatures, the temperature can be maintained to ±0.2°C during calibration.

5.3.2. Mirror Sweep Drive

Any change in temperature produces a change in the resistance of the drive coil, which in turn changes the current and the coil deflection. Hence, the mirror sweep length depends on temperature. The effect can be seen quite clearly by referring to Fig. 21, which is a spectrum of polystyrene.

The effect has been effectively eliminated by placing a combination of sensistors and resistors in the feedback circuit.

5.3.3. Temperature Gradient

During calibration a fixed temperature gradient exists between the detector and the aperture, which means that the background radiation is essentially constant. However, under field conditions the gradient might be altered, producing a significant change at some of the longer wavelengths. Our attempts to measure this effect have been unsuccessful, but a thermistor has been installed in the aperture to monitor any changes in the gradient during flight.

5.4. PRESSURE EFFECTS

5.4.1. Mirror Position

During the initial environmental tests of this instrument the sensitivity decreased as the pressure decreased. It was very difficult to determine the cause of this malfunction, but it was finally proved to be due to the motion of the mirrors. The mirrors had been fastened with Pliobond cement, which expanded slightly as the pressure decreased, tilting the optical axis away from the detector and decreasing the signal. The unit was returned to Block Associates for rework, and they installed a new drive unit which did not have this characteristic.

5.4.2. High-Voltage Arcing

The bolometer used in this instrument is operated at a relatively high bias voltage (250 volts per flake). In order to produce 250 volts across each flake, 700 volts must appear at the output of the DC-to-DC converter. This voltage produced arcing when a partial vacuum was applied to the instrument.

The problem has been eliminated by rewinding the transformer and potting

all the high-voltage components.

5.5. SIGNAL PROCESSING

5.5.1. Bolometer Time Constant

The time constant of the bolometer depends on the construction technique; for the one used in this instrument it is 1 millisecond. If the interferometer was used at the fastest sweep rate of 6 cps and at the longest sweep length 500μ, then the shorter wavelengths would be attenuated due to the slow detector response. At the sweep rate of 1.8 cps and sweep length of 250μ used in our application, the highest frequency of interest, 220 cps, is not attenuated due to the detector response.

The greatest source of noise inside the passband is amplitude fluctuations in the bias supply voltage. These fluctuations enter directly into the results and are a major factor in limiting the accuracy.

5.5.2. Amplifier

An amplitude-vs-frequency response of the total amplifier combination is shown in Fig. 22. The response is flat on the high end to 500 cps, but the low frequencies roll off at a typical rate of 6 db per octave. The lowest frequency of interest (30 cps) is down 15%.

The variation in supply voltage introduces noise in the signal. This is not as significant as the bias fluctuations due to the offsetting effects of negative feedback.

The first tube in the preamplifier has been the source of some noise trouble, and has been replaced twice during the past year. This tube was recently replaced by a ruggedized version which we hope will eliminate the problem.

5.5.3. Auxiliary Equipment

The auxiliary equipment used with the interferometer includes the telemetering, tape recorder, wave analyzer, and x-y plotter (see Fig. 23). Incorporated into the telemetering is a low-pass output filter which rolls off at 18 db per octave beyond 220 cps. Periodically during the flight, calibrate information is transmitted for the purpose of checking the auxiliary equipment. The DC calibrate signals check the sensitivity of the tape recorder, wave analyzer, and x-y plotter, and the calibrate blackbody checks the system.

5.5.4. False Signal

The sweep drive amplifier generates a large negative pulse which is not completely decoupled in the power supply. A portion of this signal ultimately appears in the output. Fortunately, all of the spectral components (Fig. 24) due to this false signal fall outside the normal spectral range.

When the power is removed, the loop tape recorder used for the wave analyzer data reduction generates a noise pulse which reduces the effectiveness of this method of data reduction. Fortunately the pulse occurs at a regular rate, so that it can be partially separated from the signal.

5.5.5. Error Summary

Typical wave number calibration curves are shown in Fig. 25. The probable error is not a constant, but varies with both temperature and wave number. The range is from 1°C to 10°C.

As a check on the reliability of the data, the blackbody (Fig. 26) will be monitored at regular intervals during the flight. Since the blackbody temperature is measured directly, the correspondence between the interferogram data and the thermistor will be a direct measure of the error. This same technique has been applied in the laboratory. The results (Fig. 27) are a direct measure of the accuracy of the instrument as a function both of wave number and of target temperature.

Two sets of data have been included. The first (Fig. 27A) is data which was taken simultaneously with the calibration data. In this case the bolometer temperature was fixed and there was no error due to interpolating the bolometer temperature. Also any unknown errors associated with the calibrating apparatus would tend to be cancelled. This setup represents the very best possible results.

The second set (Fig. 27B) is data taken with a completely different setup. No attempt was made to control the bolometer temperature, which varied through the run. This is typical operation and the errors should be considered as typical.

6. OVERALL SUMMARY

6.1. INSTRUMENT MALFUNCTION

The overall progress on this project has been plagued by three instrument malfunctions: (1) use of Pliobond cement to fasten the mirror, (2) high-voltage breakdown, and (3) an intermittently noisy pre-amplifier tube. But since none of these items are fundamental to the I-4 in particular, they must be ignored in any final evaluation of the instrument.

6.2. ENGINEERING DESIGN

An engineering evaluation based on how closely the factors affecting response, resolution, and required bandwidth are matched shows that the design is good.

Low frequency Limit	Amplifier 30 cps—equivalent to	15.2μ
	Window	15μ
	Beam splitter and compensator	15μ
High Frequency Limit	Filter 220 cps—equivalent	2μ
	Beam splitter (germanium)	2μ
	Acceptance angle	3.75μ
Resolution Limit	Mirror displacement	40 cm^{-1}
	Acceptance angle	40 cm^{-1} at 3.75μ
	Mirror drive linearity	40 cm^{-1} at 7μ

One factor which should be improved is the linearity of the mirror drive.

The probable error given in Fig. 25 is determined primarily by the noise generated during the data reduction process. Hence, the signal-to-noise ratio of the instrument itself is satisfactory.

6.3. CALIBRATION

The calibration techniques and equipment which have been developed during this program are adequate for this instrument.

In the future we plan to make greater use of the vacuum calibrator. It has several advantages:

1) Atmospheric absorption is no problem.

2) Thermal insulation is relatively effective.

3) Liquid nitrogen cooling is relatively easy.

Its disadvantages are that:

1) Space is at a premium.

2) Normally manipulation inside the vacuum system is not possible.

6.4. FUTURE DEVELOPMENTS

6.4.1. Ground Measurements

Our present plans are to use the interferometer to make atmospheric measurements from the ground. Observation of the sky under various atmospheric conditions will provide practice in reducing data, and the data can be compared with that obtained by other workers.

6.4.2. Balloon Flight Tests

The interferometer will be flown on a high altitude balloon in conjunction with the Tiros and Nimbus 5-channel radiometers. Periodically during the flight all three instruments will be pointed in the same direction for comparison purposes. The interferometer will not have the spatial resolution of the radiometers, but comparison of the data whould be satisfactory for many targets.

6.4.3. Emissivity Measurements

We are planning an experiment in which we will use the interferometer to measure the emissivity of paint samples and the effect of geometric shape on emissivity. These measurements will be compared with results obtained with other equipment.

6.4.4. Design Development

The following developments are now being considered:

1) The incorporation of a scanning mirror to permit a 200° scan past both horizons.

2) The addition of a small Cassegrainian telescope to increase the spatial resolution.

3) The development of an improved mirror drive to be used in a future higher-resolution instrument.

4) The investigation of an analog computer for data reduction. It is technically feasible to reduce the data in real time and to continuously plot temperature as a function of wave number.

7. ACKNOWLEDGMENT

The research described in this report was initiated in November, 1961 as the result of a suggestion by Dr. G.B.B.M. Sutherland that interferometry be investigated as an atmospheric radiation measurement technique. The success of the research was dependent on the efforts of many persons, particularly, D. A. Robinson who carried out many of the calibrations and instrument modifications, and M. G. Kakli who performed the data reduction. Thanks also go to F. L. Bartman for encouragement and support and for editing the manuscript and to M. T. Surh for his contribution to the data analysis.

We are grateful to the National Aeronautics and Space Administration for the financial support which made this effort possible. The work was started under Contract NASw-140, which has since been superseded by Contract NASr-54(03).

8. REFERENCES

1. Strong, J., Interferometry in the Far Infrared, J. Opt. Soc. Am., 47, 354-357, 1957.

2. Strong, J. and Vanasse, G. A., Interferometric Spectroscopy in the Far Infrared, J. Opt. Soc. Am., 49, 844-850, 1959.

3. Gebbie, H. B., Michelson Interferometry and Numerical Fourier Transformation, Nat. Phys. Lab., Symposium 11, 425-430, June 1959.

4. Felgett, P. B., J. Phys. Radium, 19, 149, 1958.

5. Ballard, S. S., McCarthy, K. A. and Wolfe, W. L., Optical Materials for Infrared Instrumentation, The University of Michigan Willow Run Labs. Report, January 1959.

6. Barnes Engineering, Calibration and Test Data for 5-Channel Satellite Radiometer, May 18, 1961.

7. Barnes Engineering, Thermistor Flake Coatings, Report 4870-02.

8. Chaney, L. W., "Thermal Radiation Calibrator for TIROS MRIR Radiometer," The University of Michigan ORA Report 05863-4-T, in process.

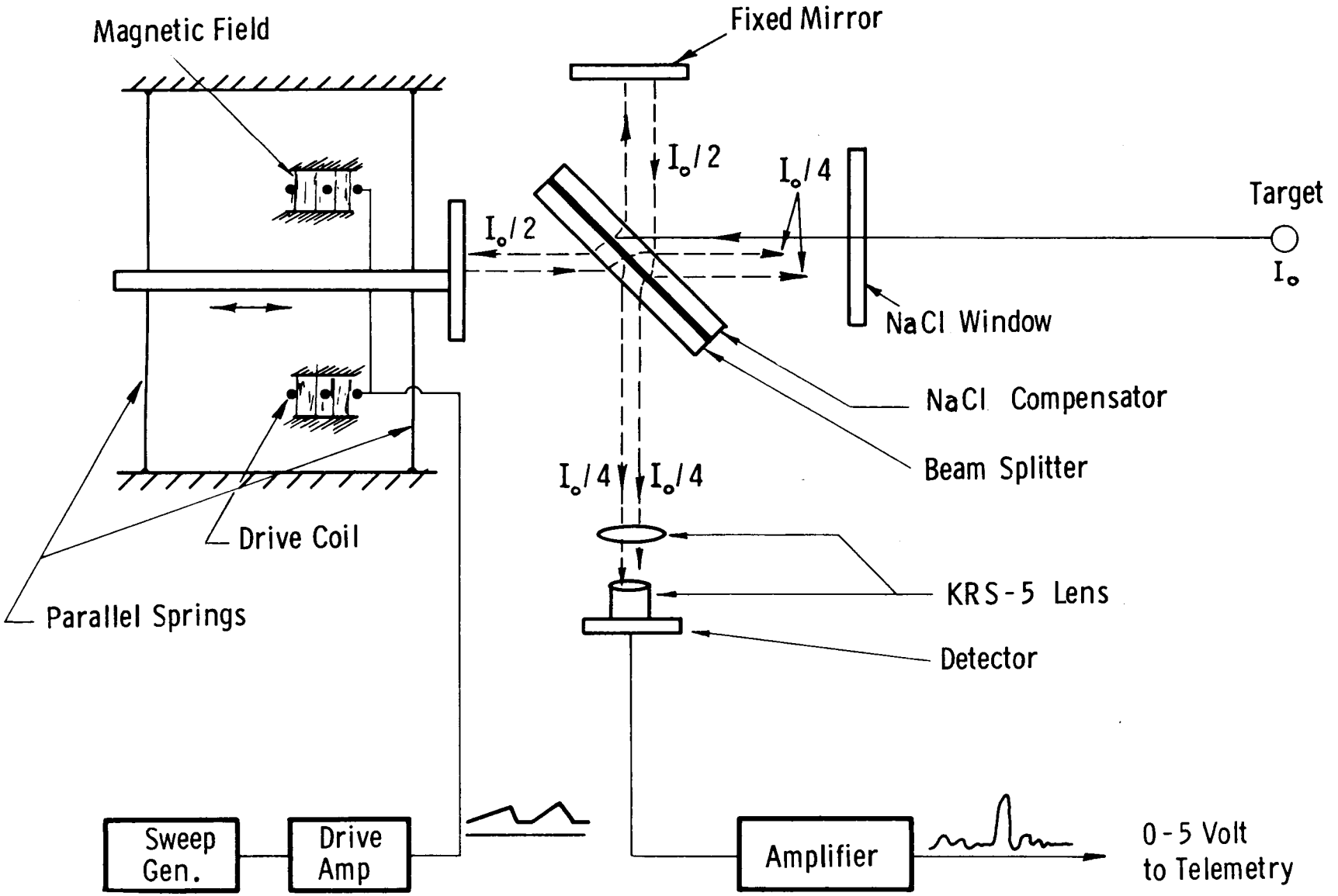

Fig. 1. Interferometer (block diagram).

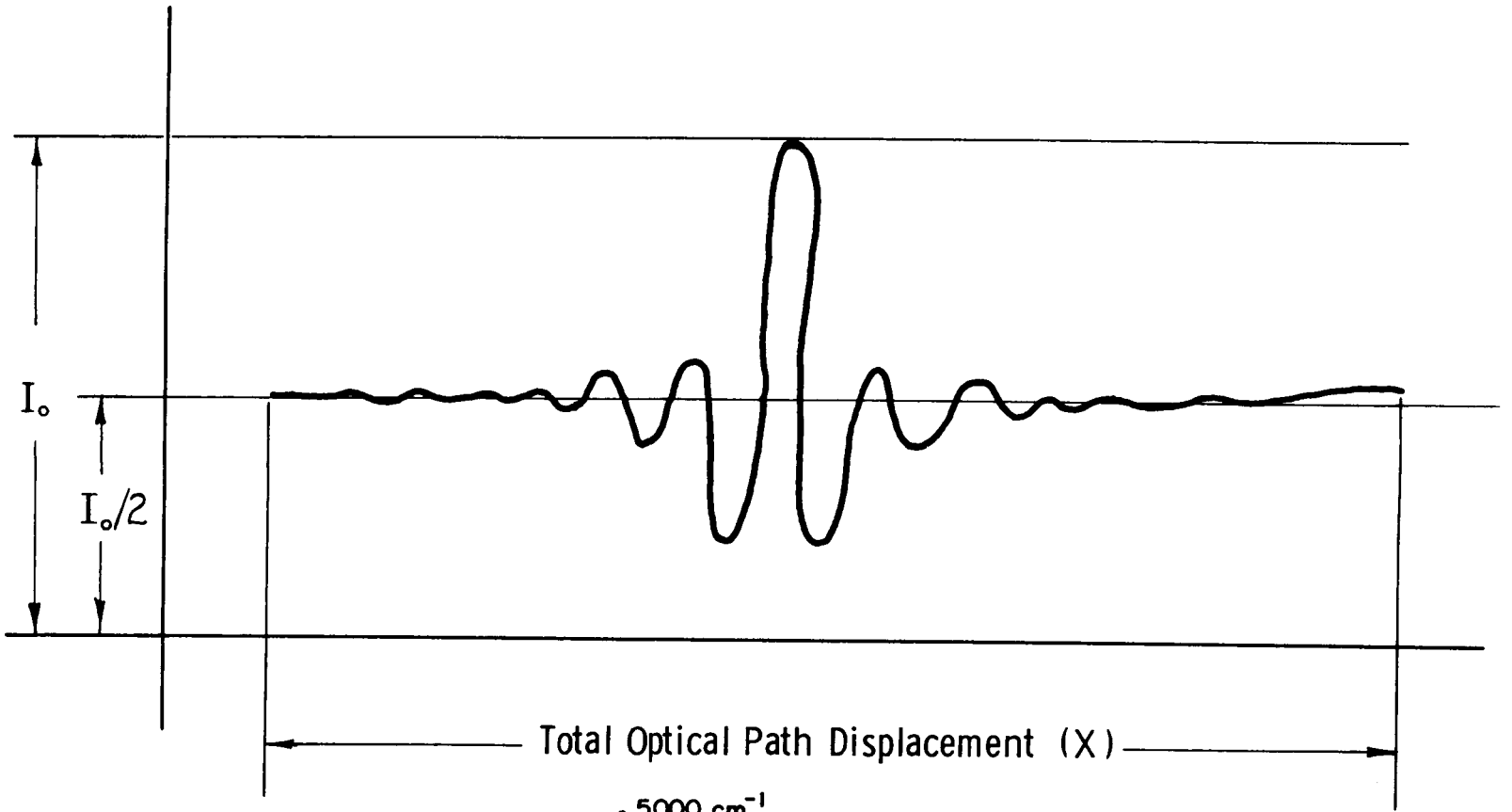

$$I(x) = \int_{560\ cm^{-1}}^{5000\ cm^{-1}} I(\nu)/2 \cos 2\pi \nu x \, d\nu$$

Fig. 2. Interferogram

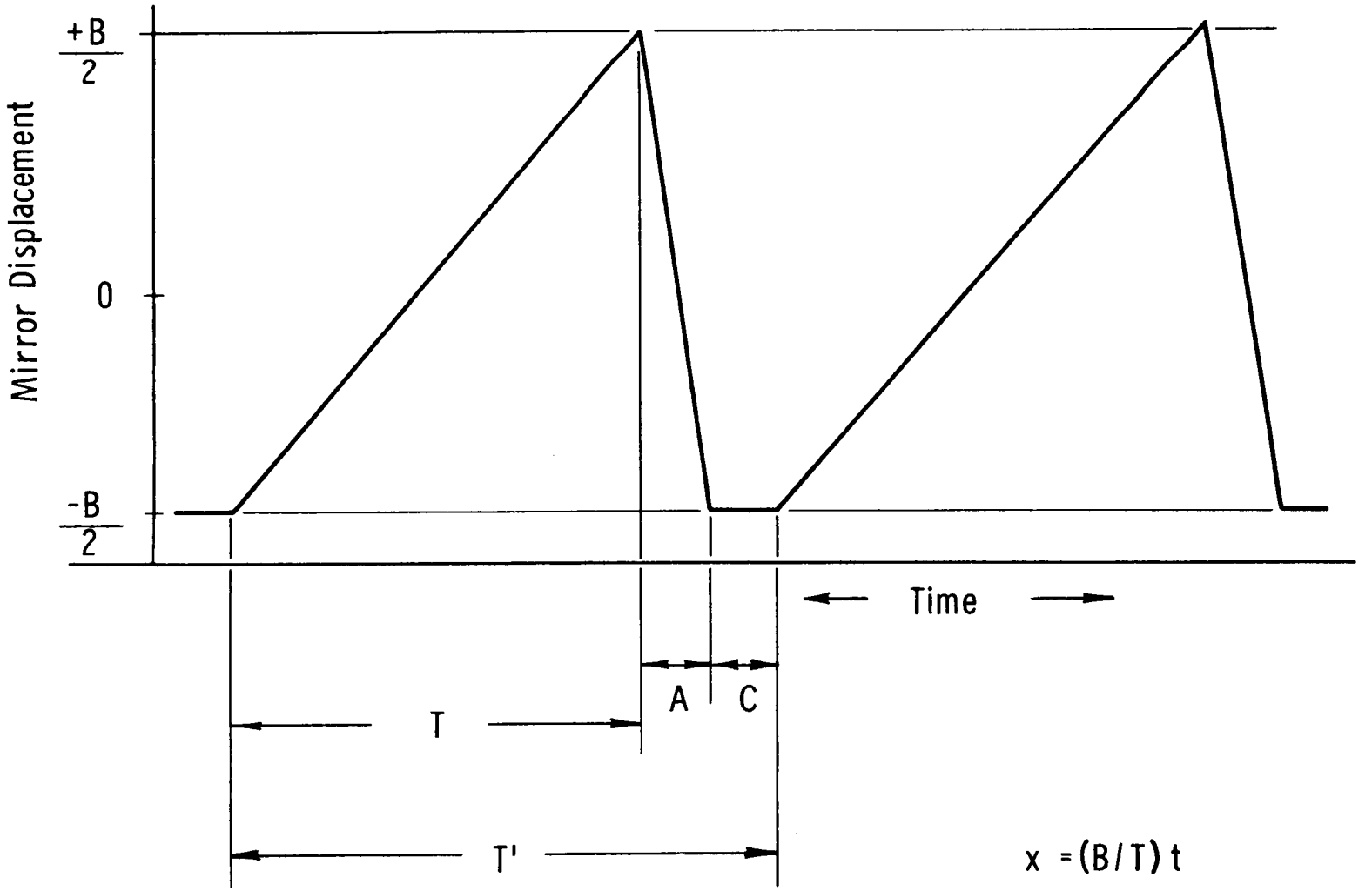

Fig. 3. Mirror displacement vs time.

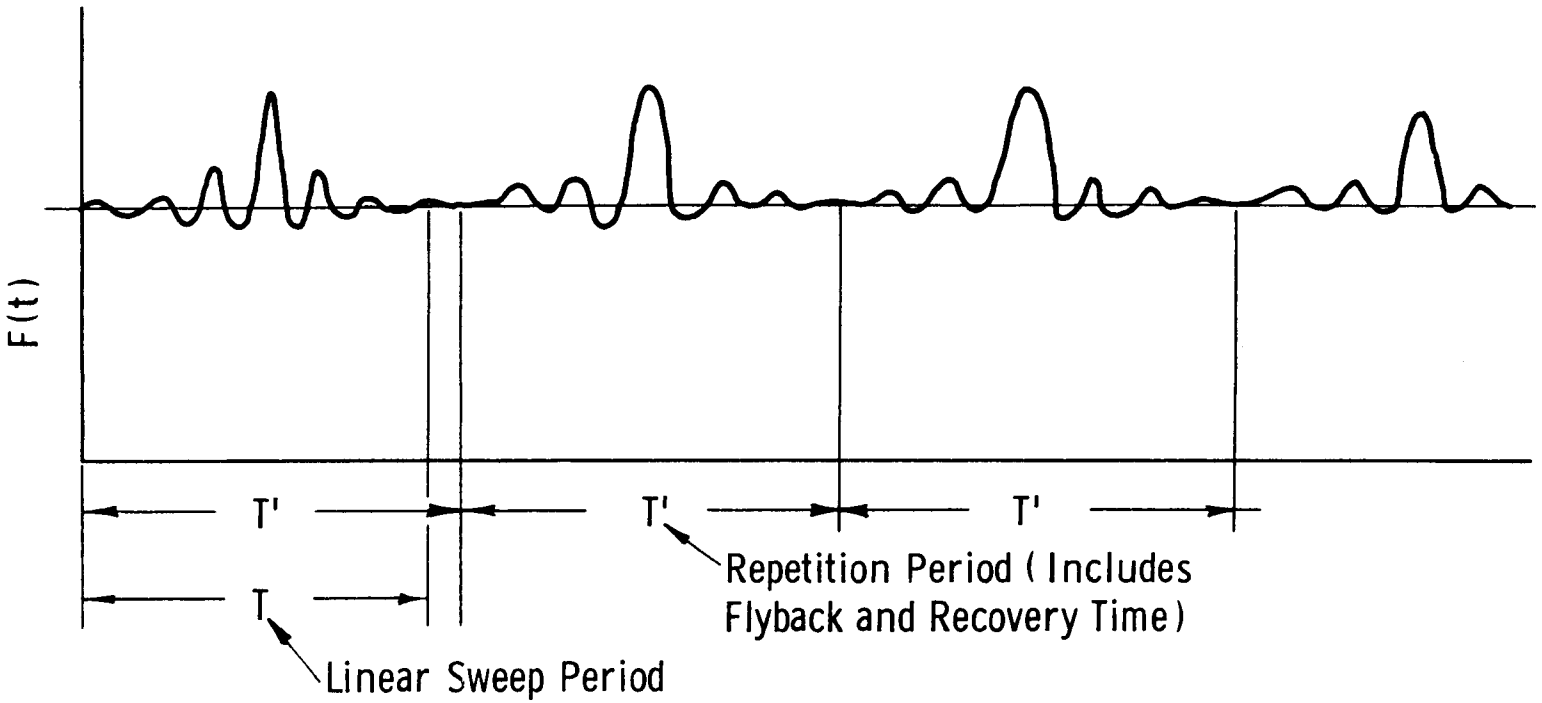

Fig. 4. Interferogram repetitive function.

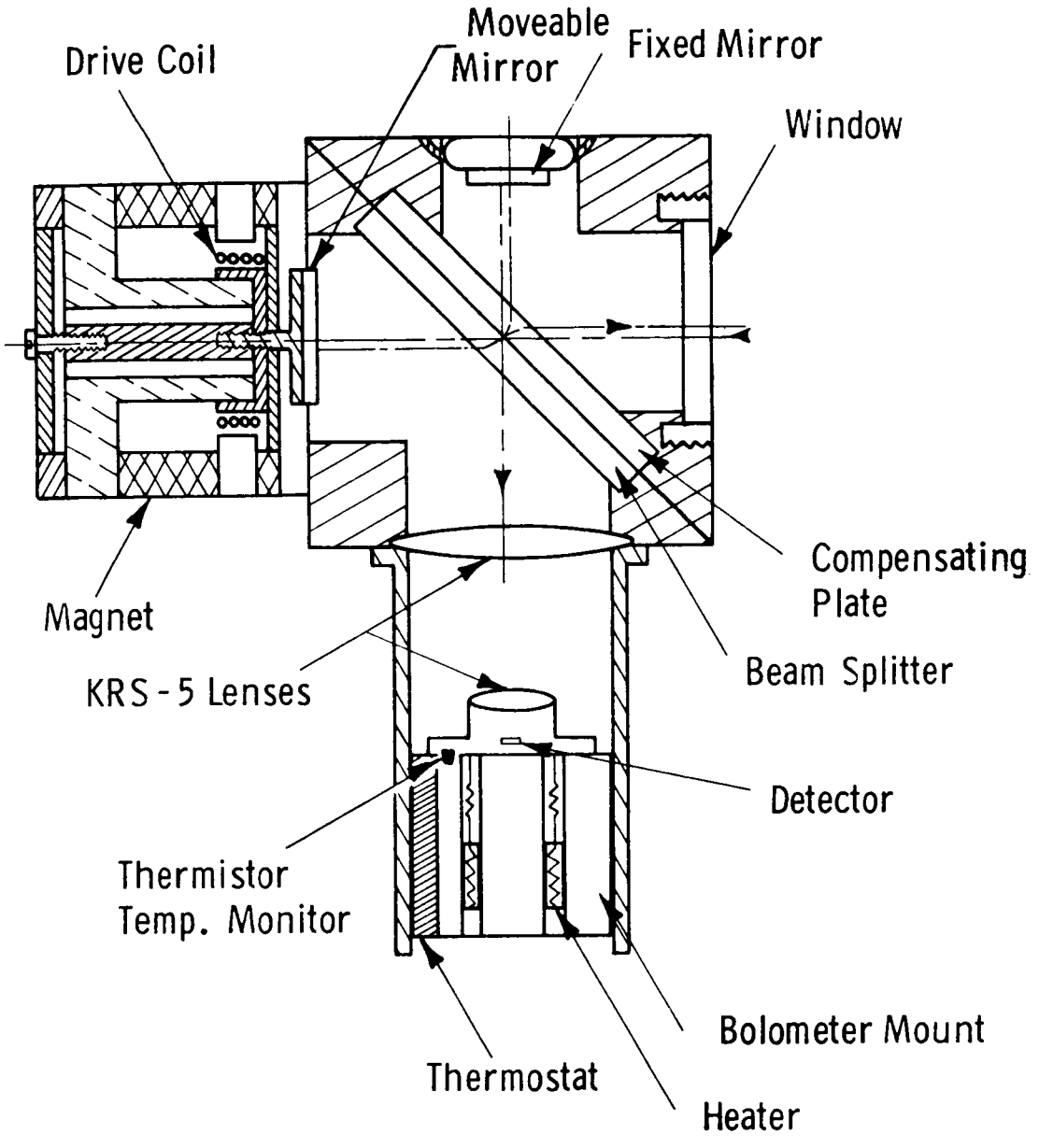

Fig. 5. Cube optics.

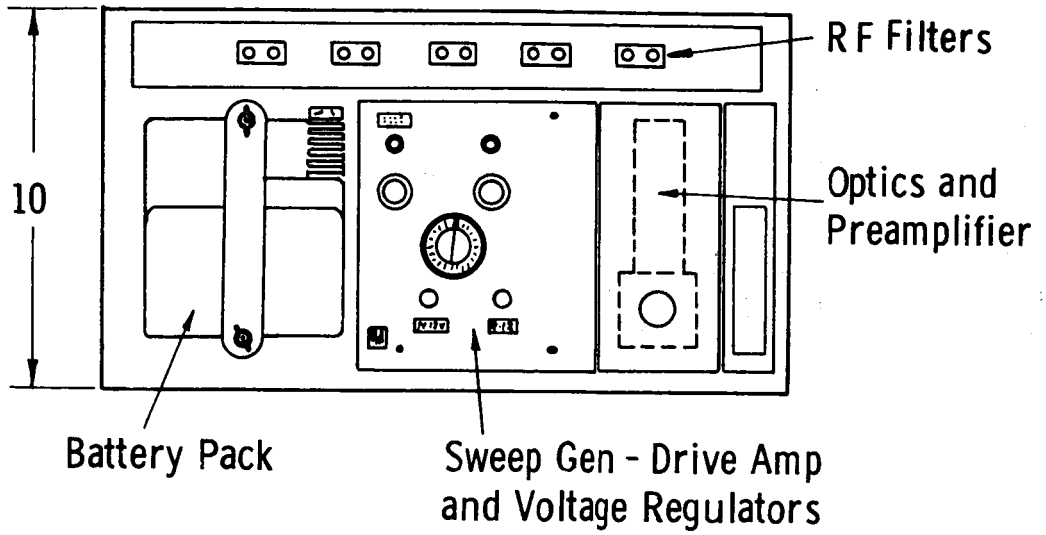

(a) Top View

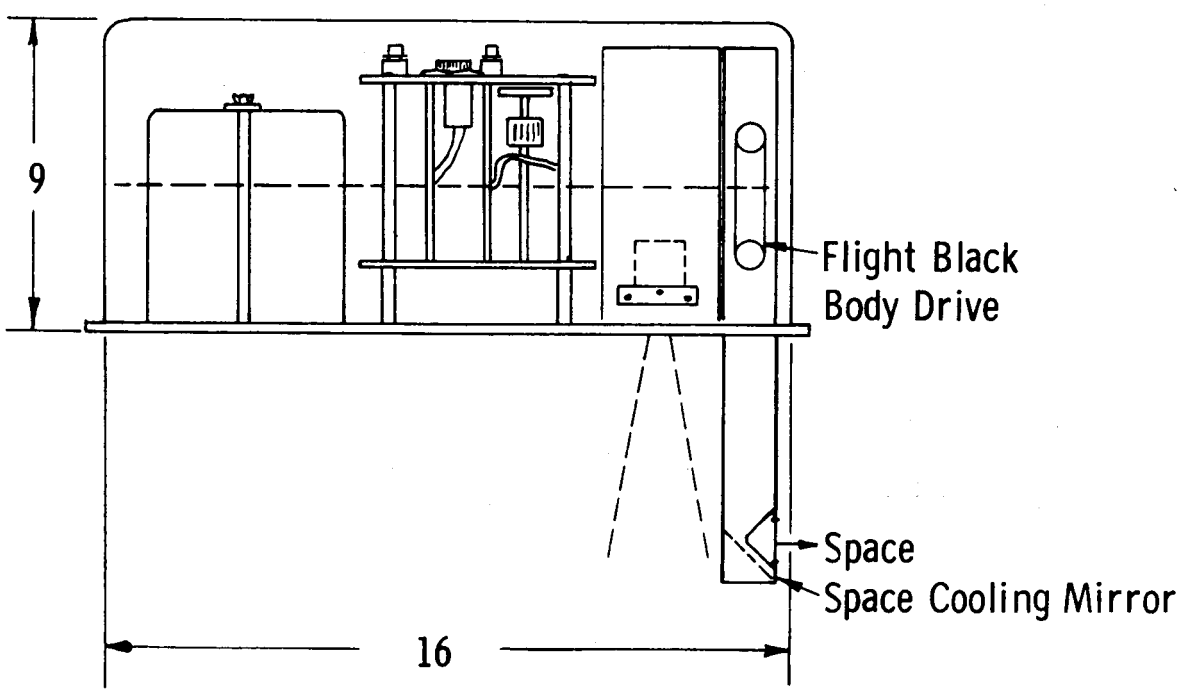

(b) Side View

Fig. 6. Assembly drawing: (a) Top view, (b) Side view.

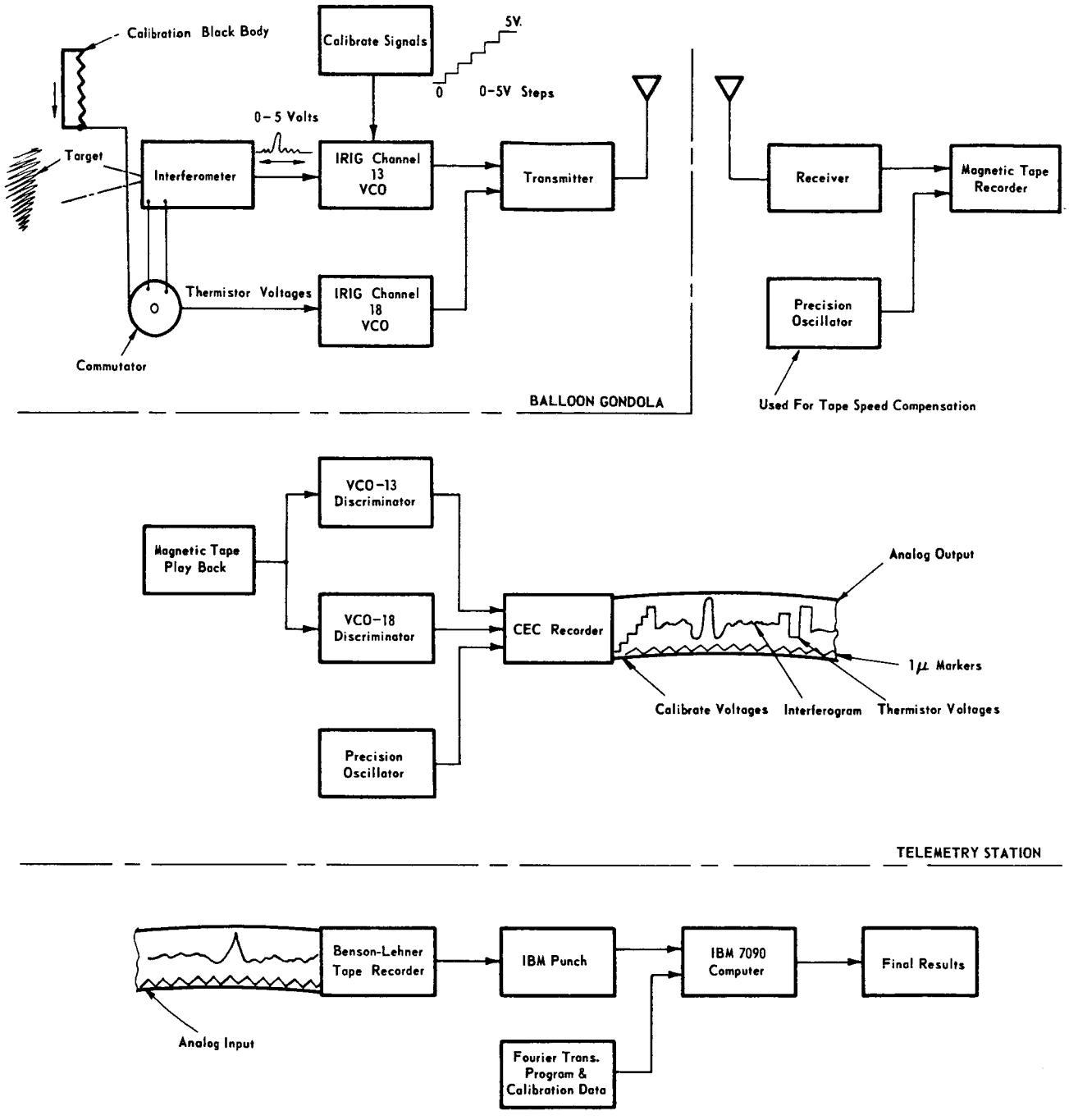

Fig. 7. Digital data reduction (block diagram).

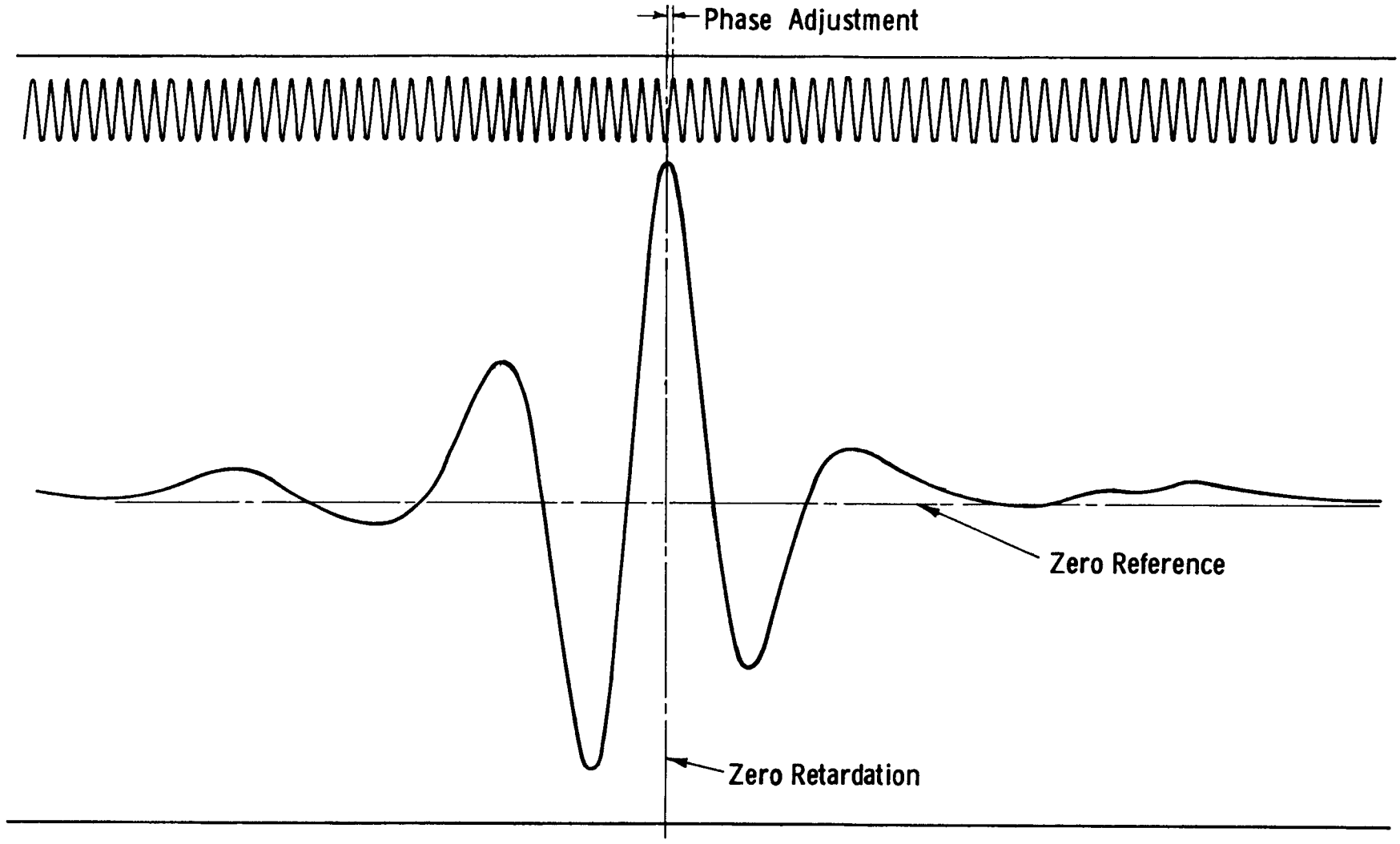

Fig. 8. Typical CEC recording of interferogram.

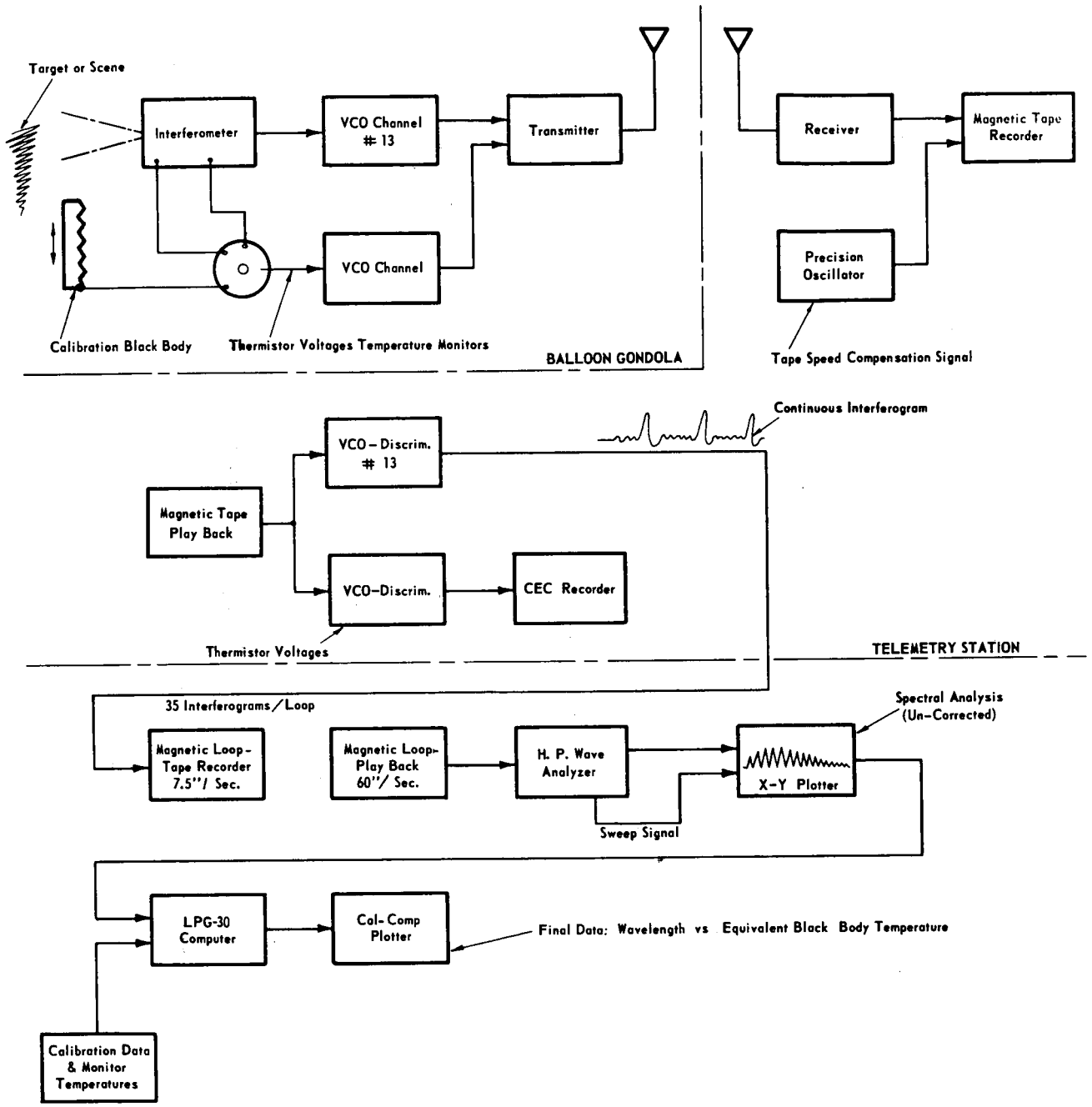

Fig. 9. Wave analyzer data reduction (block diagram).

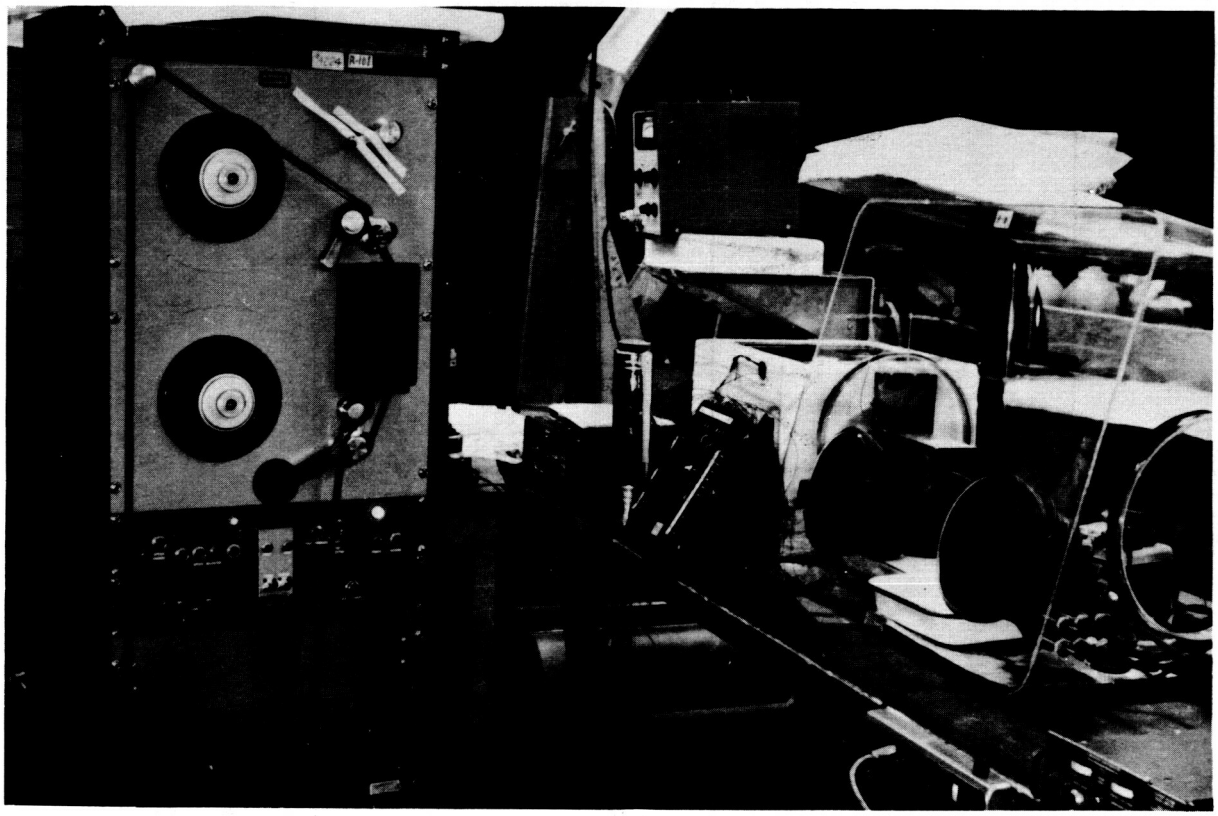

Fig. 10. Loop tape recorder (photograph).

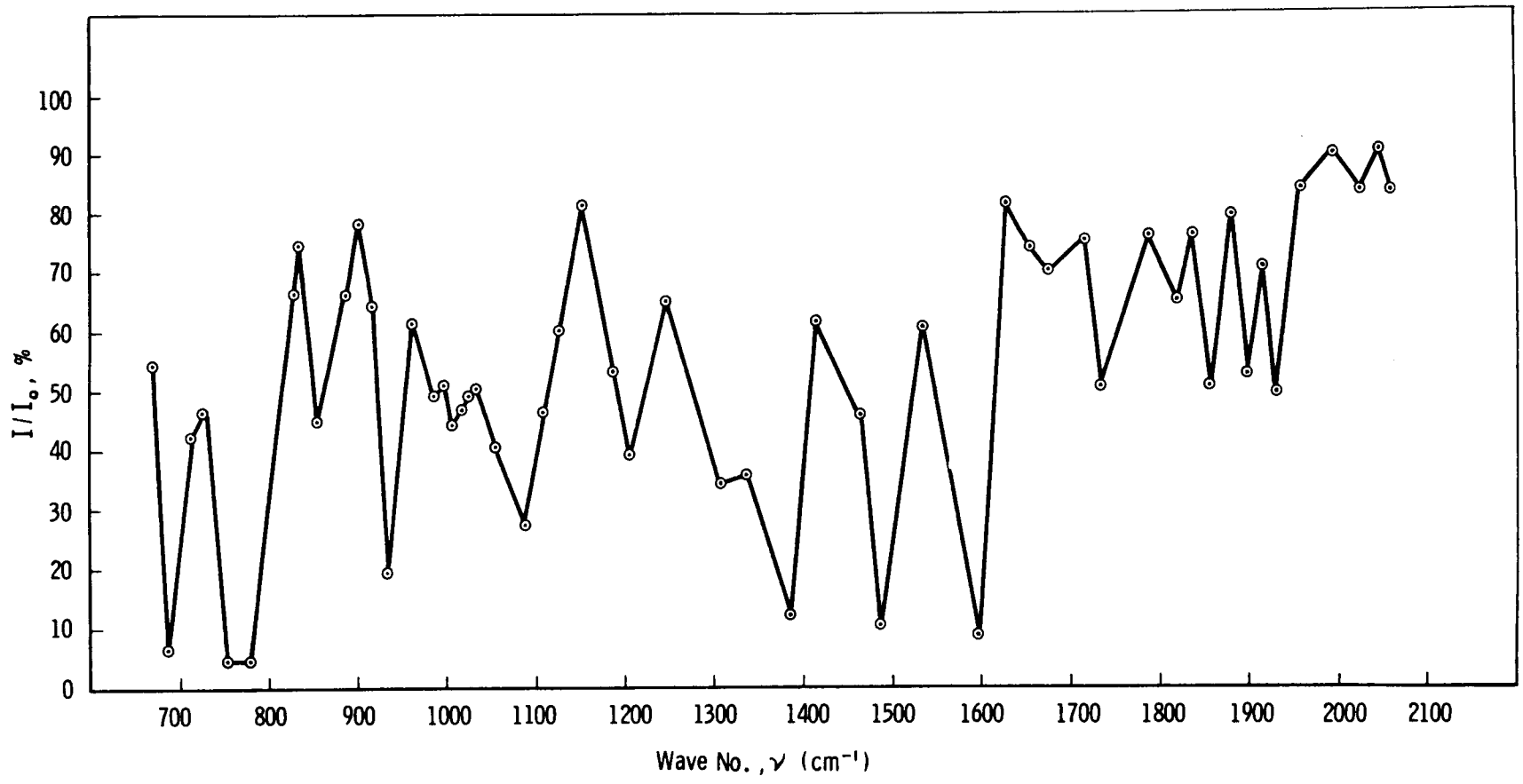

Fig. 11. Polystyrene spectra.

	Block Assoc. Values	Sweep Frequency, cps			
		5.9	3.36	1.78	0.92
	Using 3μ Spike Filter in Front of Optics				
1	61μ	83μ	71.5μ	64.5μ	54.3μ
2	122	165	146	132	120
3	245	327	297	270	244
4	492	661	575	534	510
	Using 5μ Narrow Band Filter				
1	61	85μ			
2	122		146μ		
3	245			271μ	
4	492				517μ

Fig. 12. Optical path calibrations vs sweep frequency.

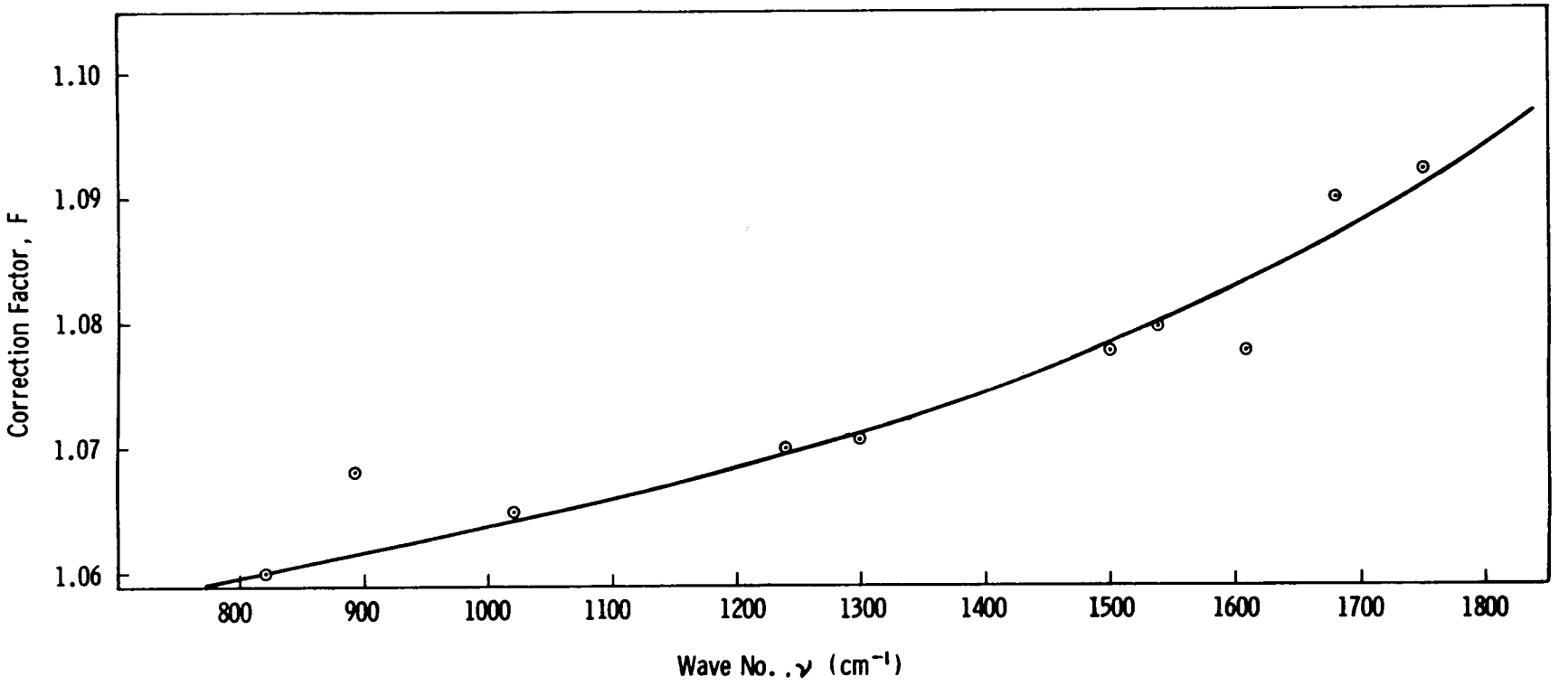

Fig. 13. Wavelength calibration curve.

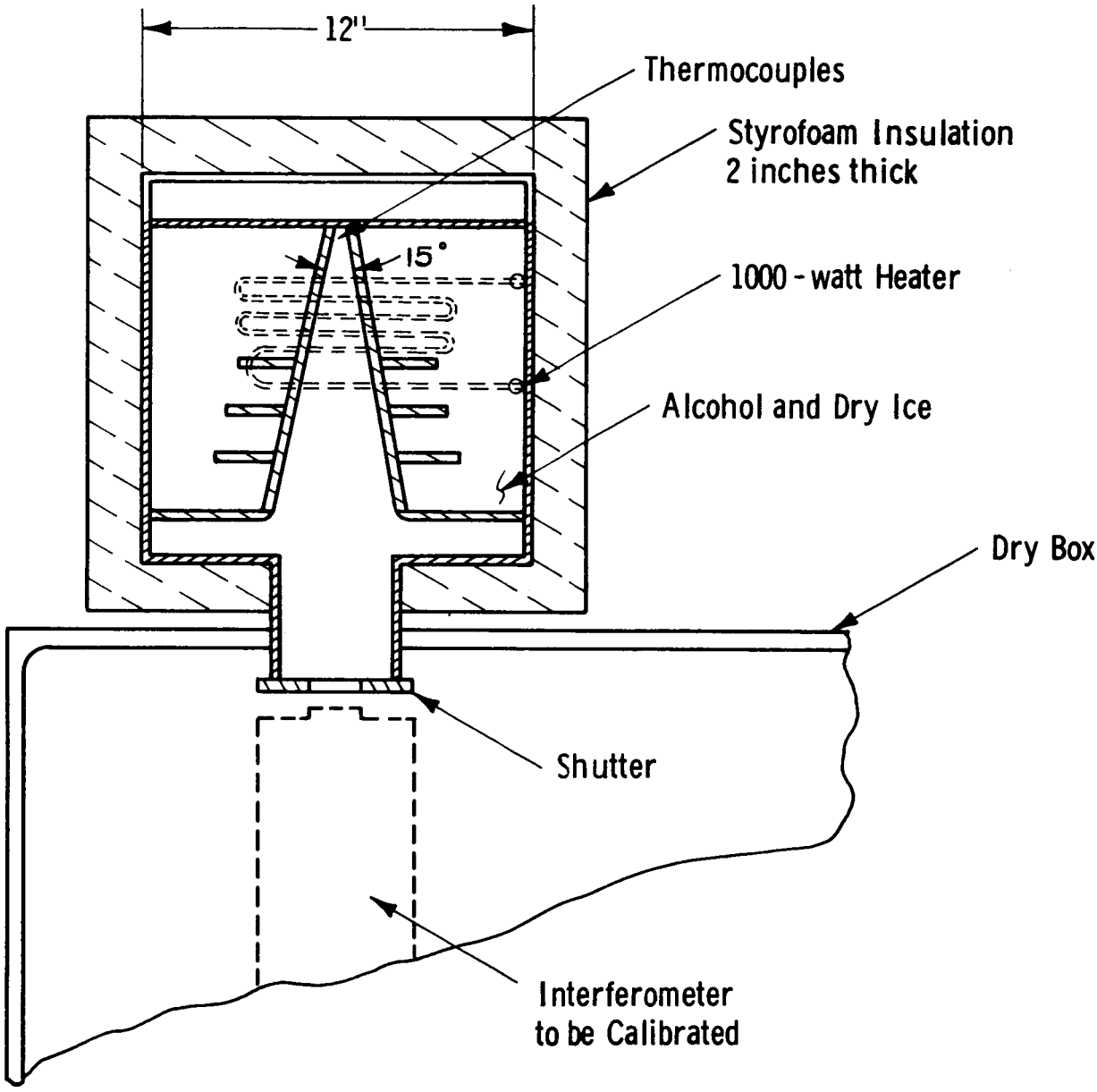

Fig. 14. Low-temperature calibration equipment (diagram).

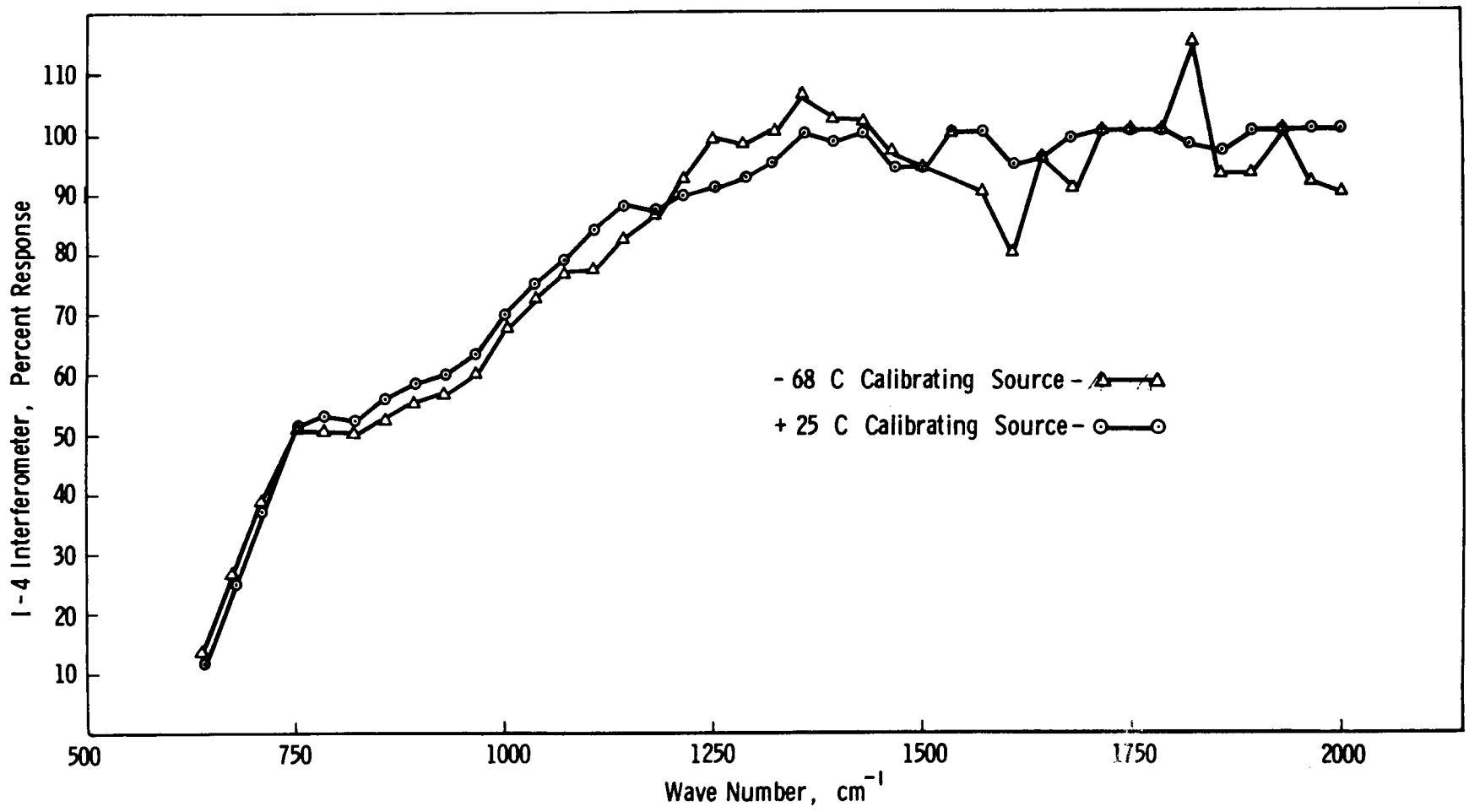

Fig. 15. Instrument spectral response.

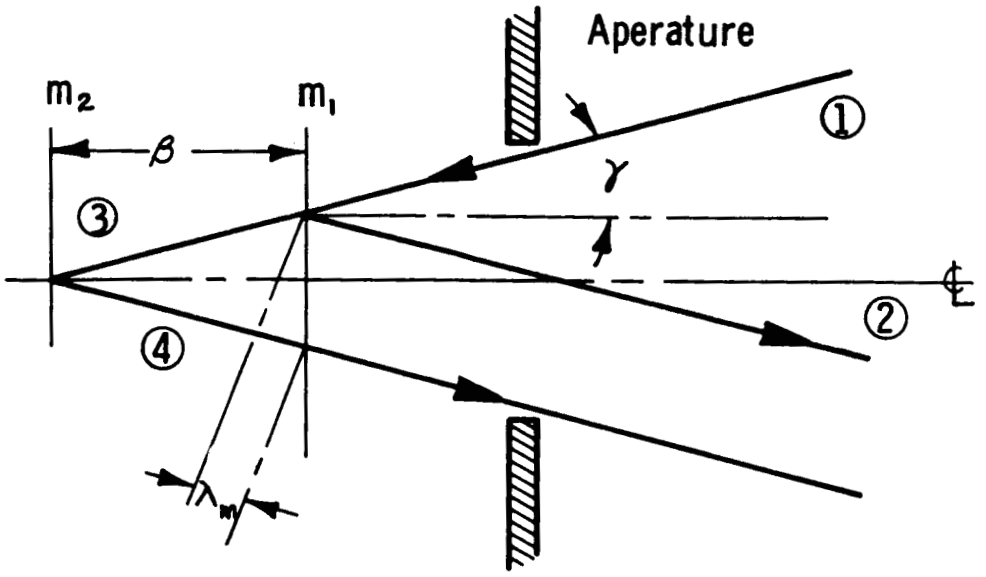

(Minimum Wavelength) $\lambda_m = 2\gamma^2\beta$

(Maximum Wave Number) $\nu_m = \frac{1}{\lambda_m}$

Resolution $\Delta\nu = \frac{1}{2\beta}$

Fig. 16. Light path divergence.

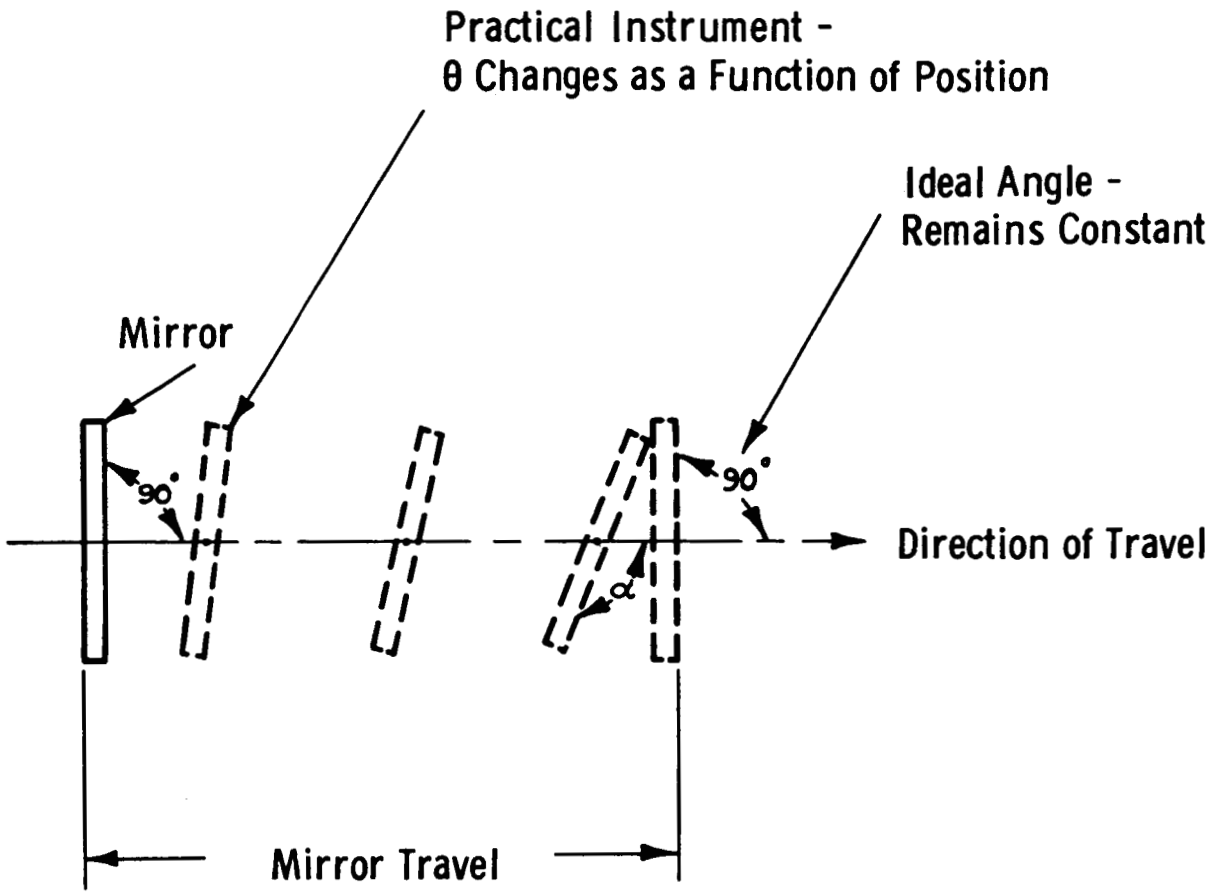

Fig. 17. Mirror rotation.

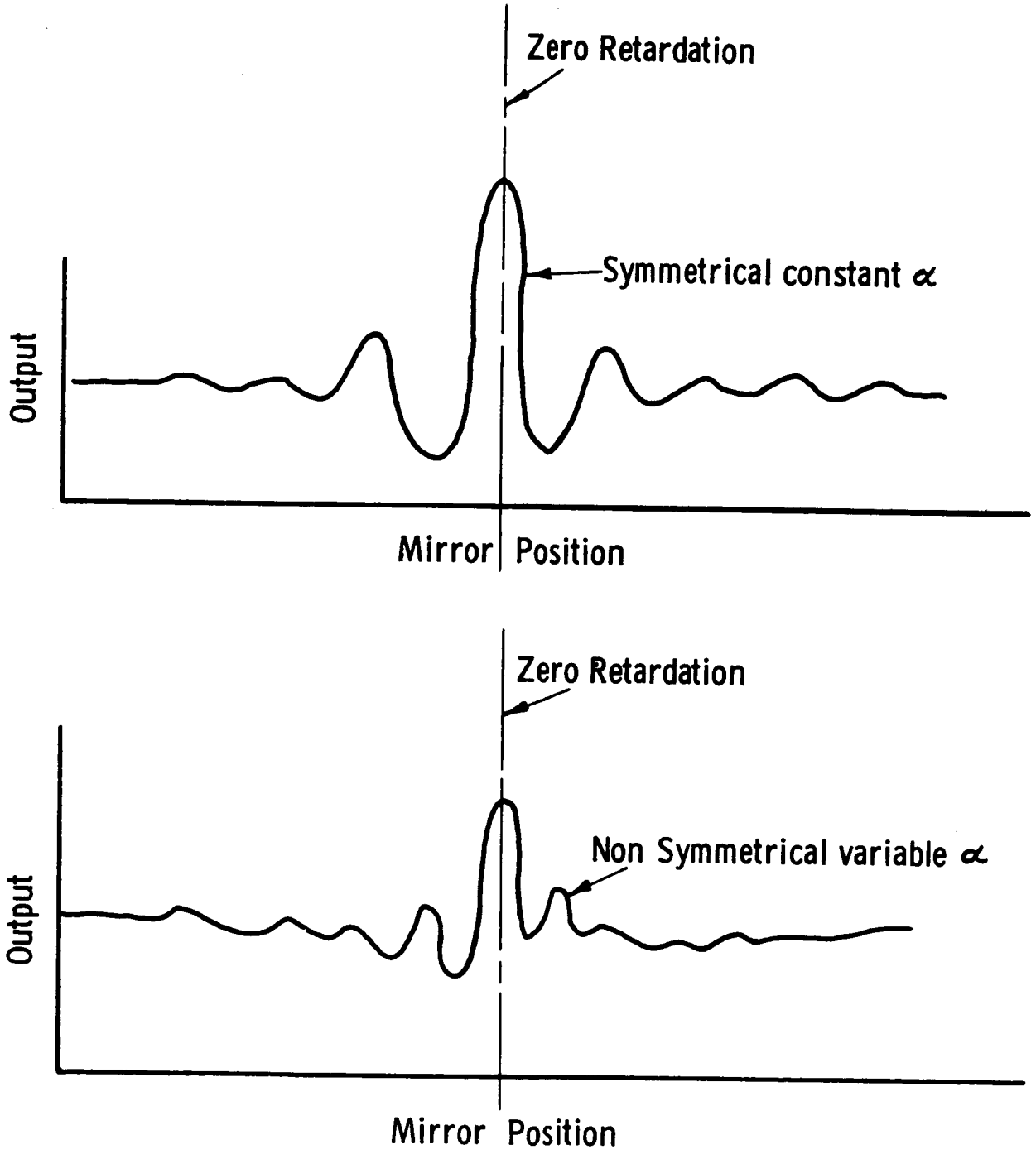

Fig. 18. Interferogram, symmetric and nonsymmetric.

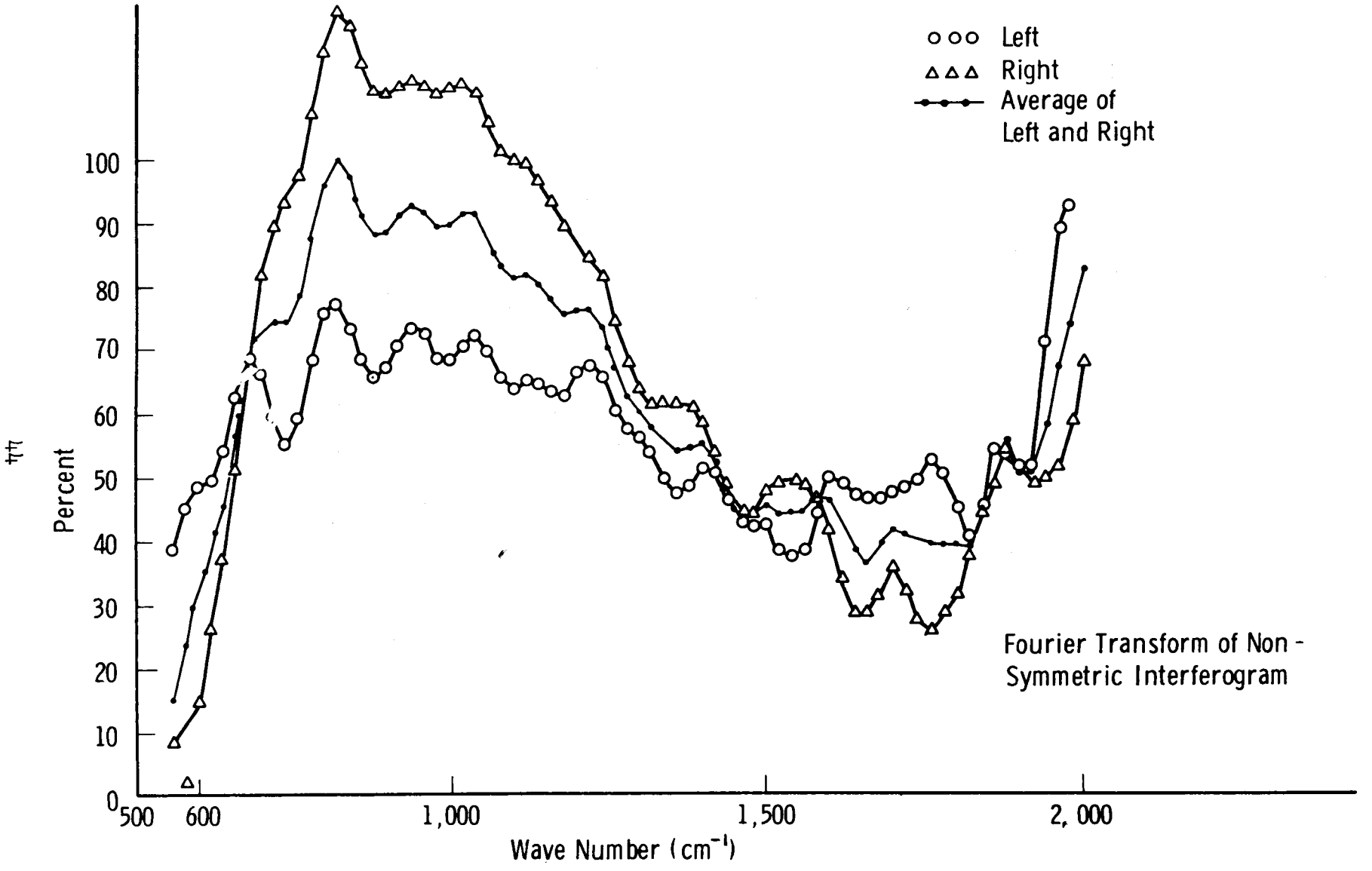

Fig. 19. Fourier transform of nonsymmetric interferogram.

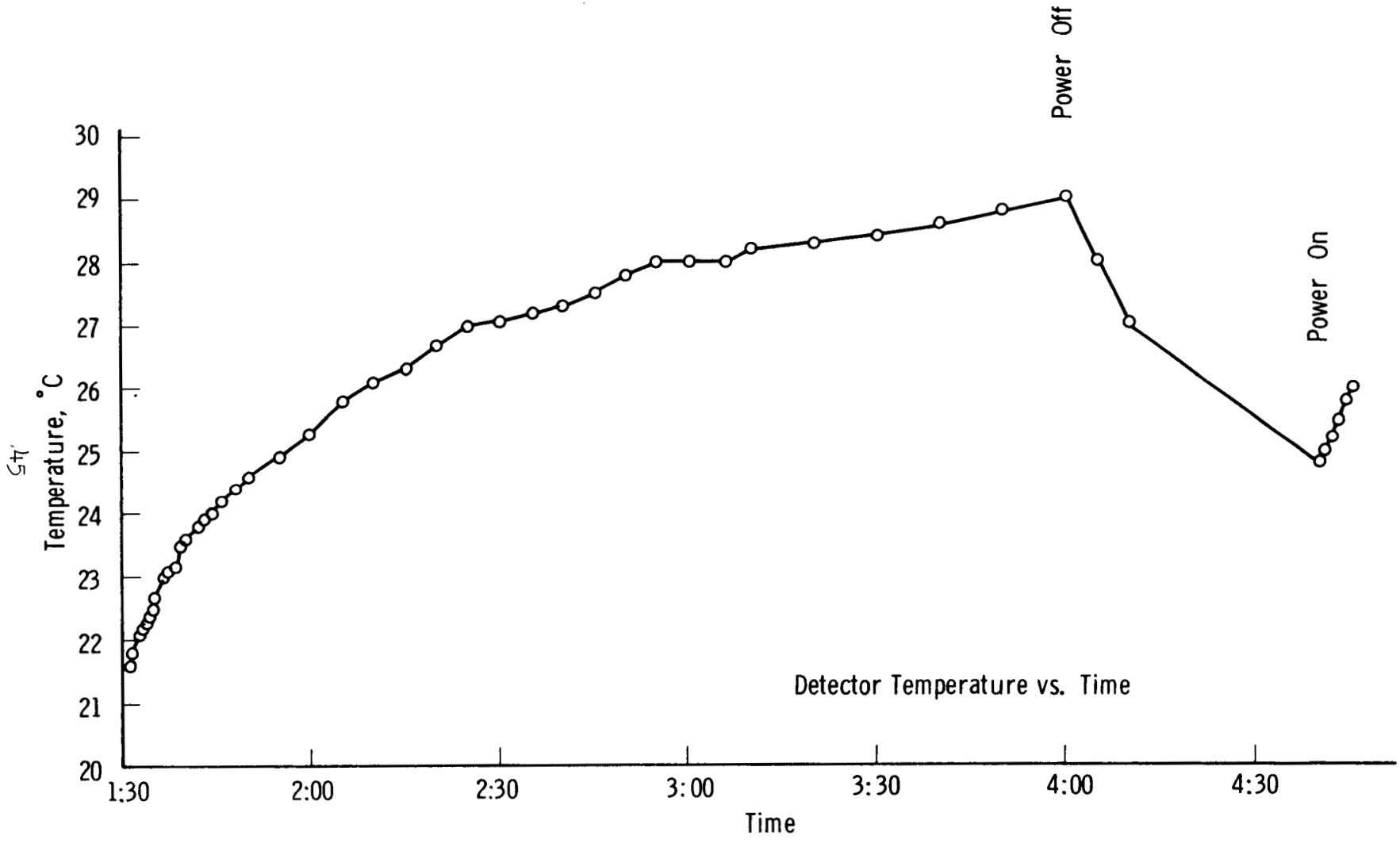

Fig. 20. Detector temperature vs time.

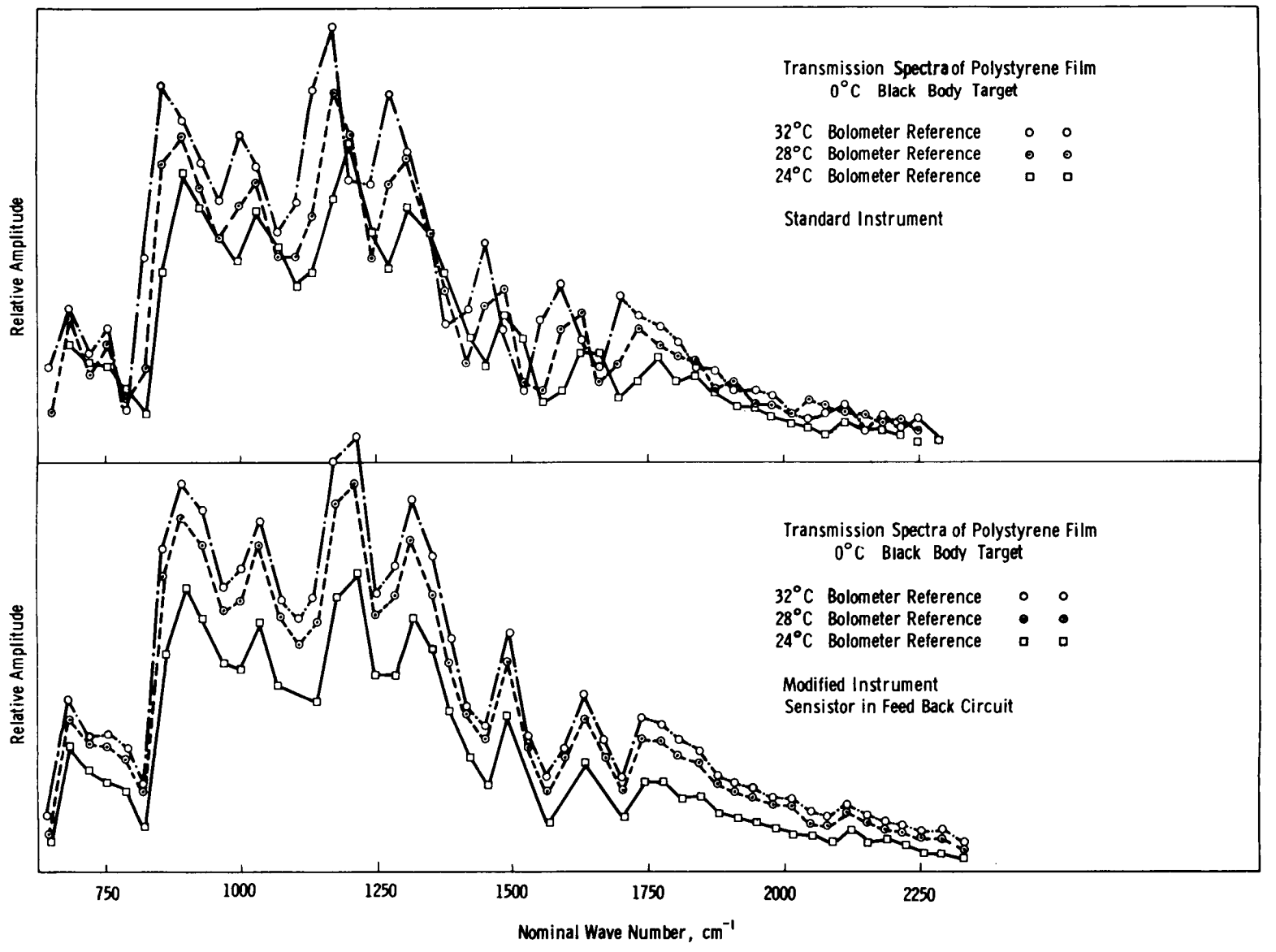

Fig. 21. Effect of temperature-induced sweep length variation.

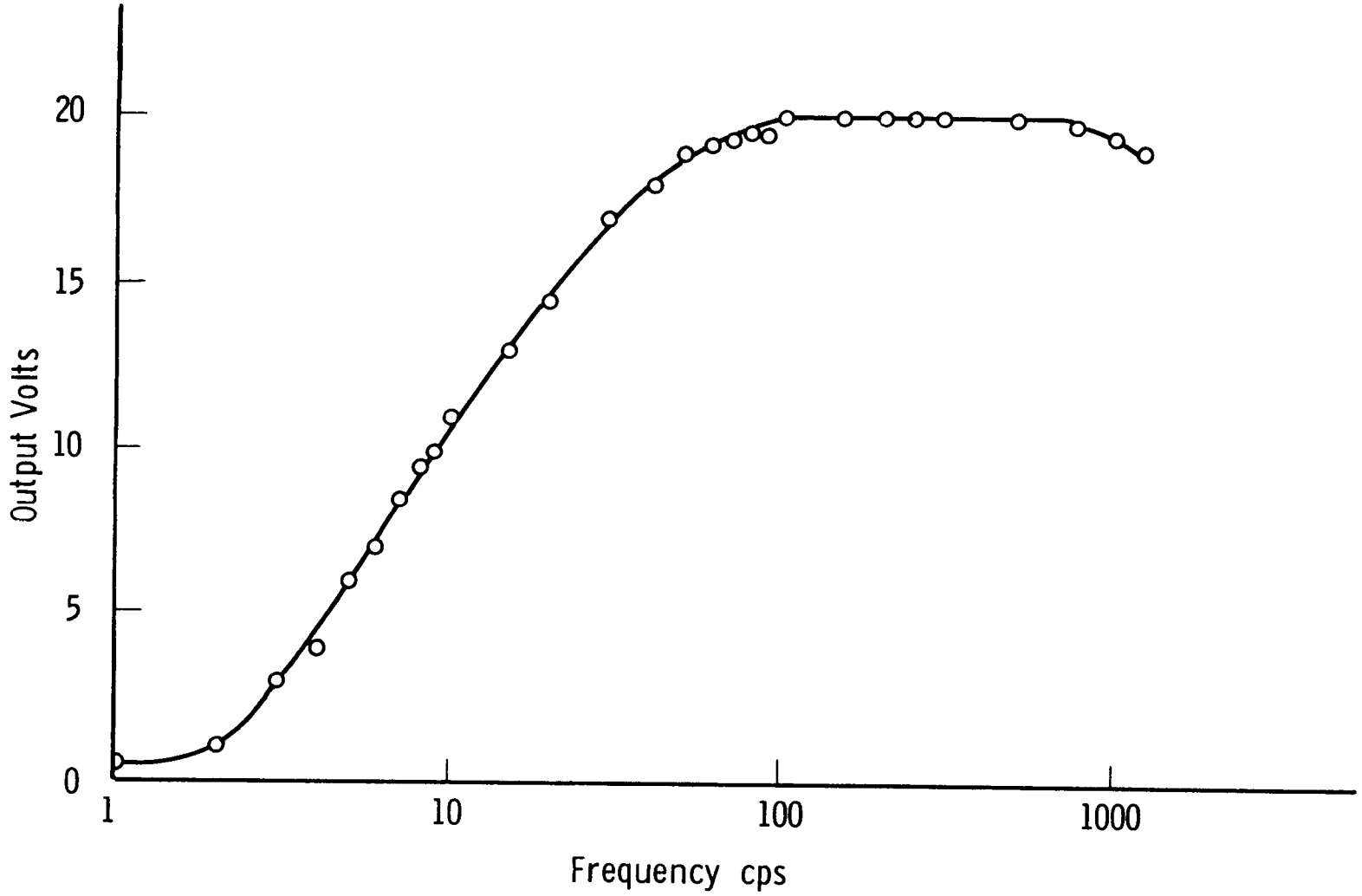

Fig. 22. Amplifier response.

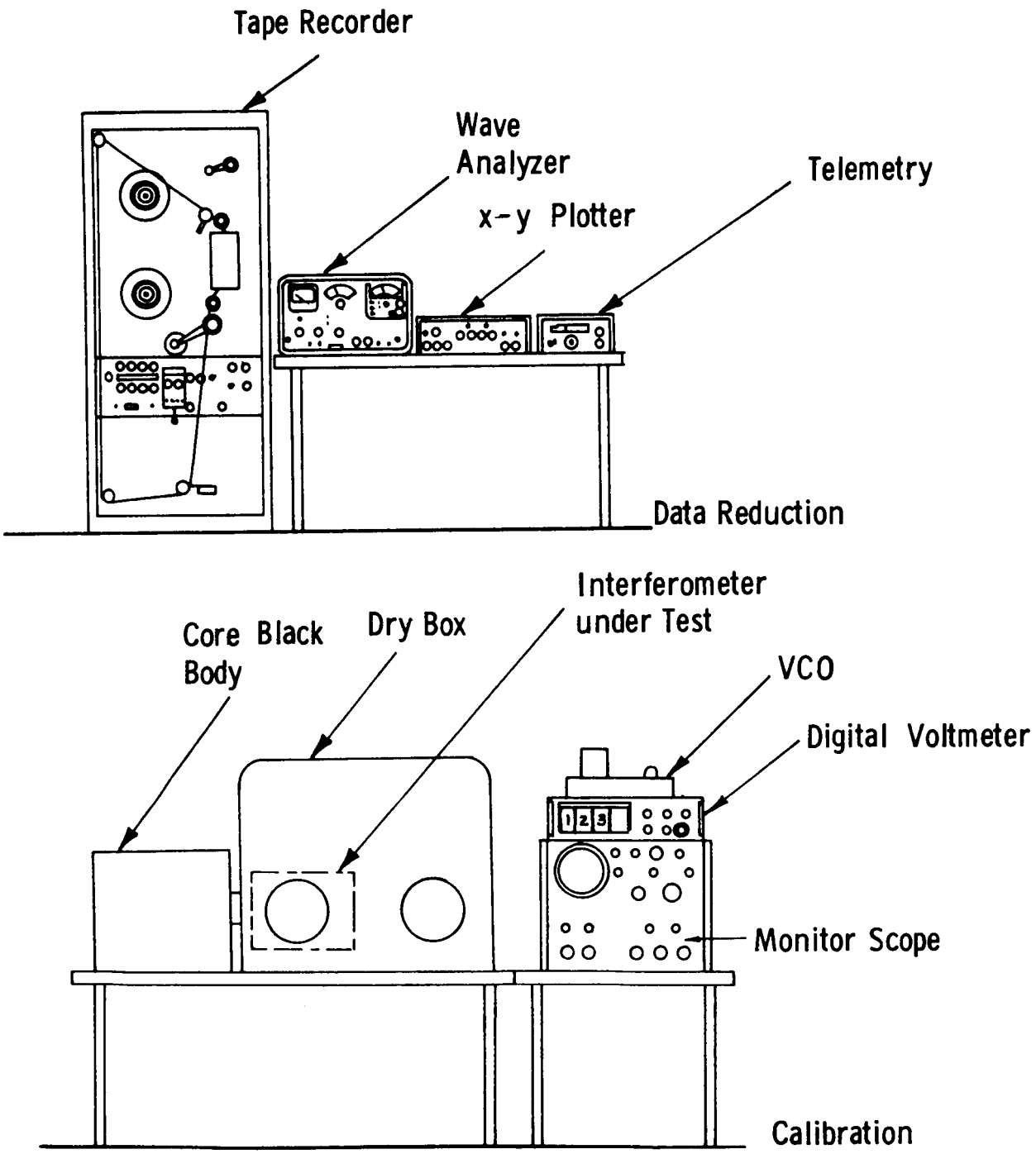

Fig. 23. Auxiliary equipment (diagram).

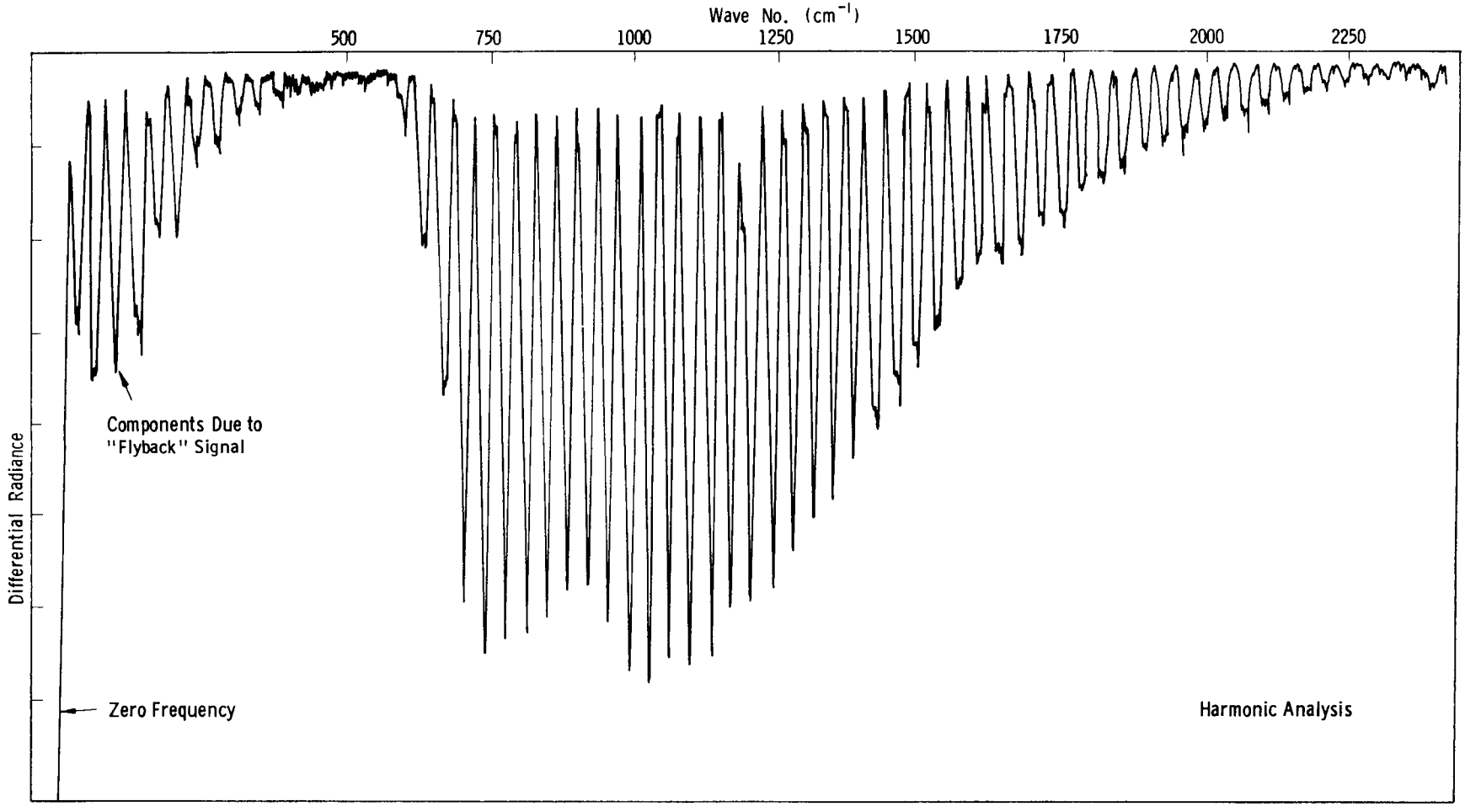

Fig. 24. Harmonic analysis, including zero frequency.

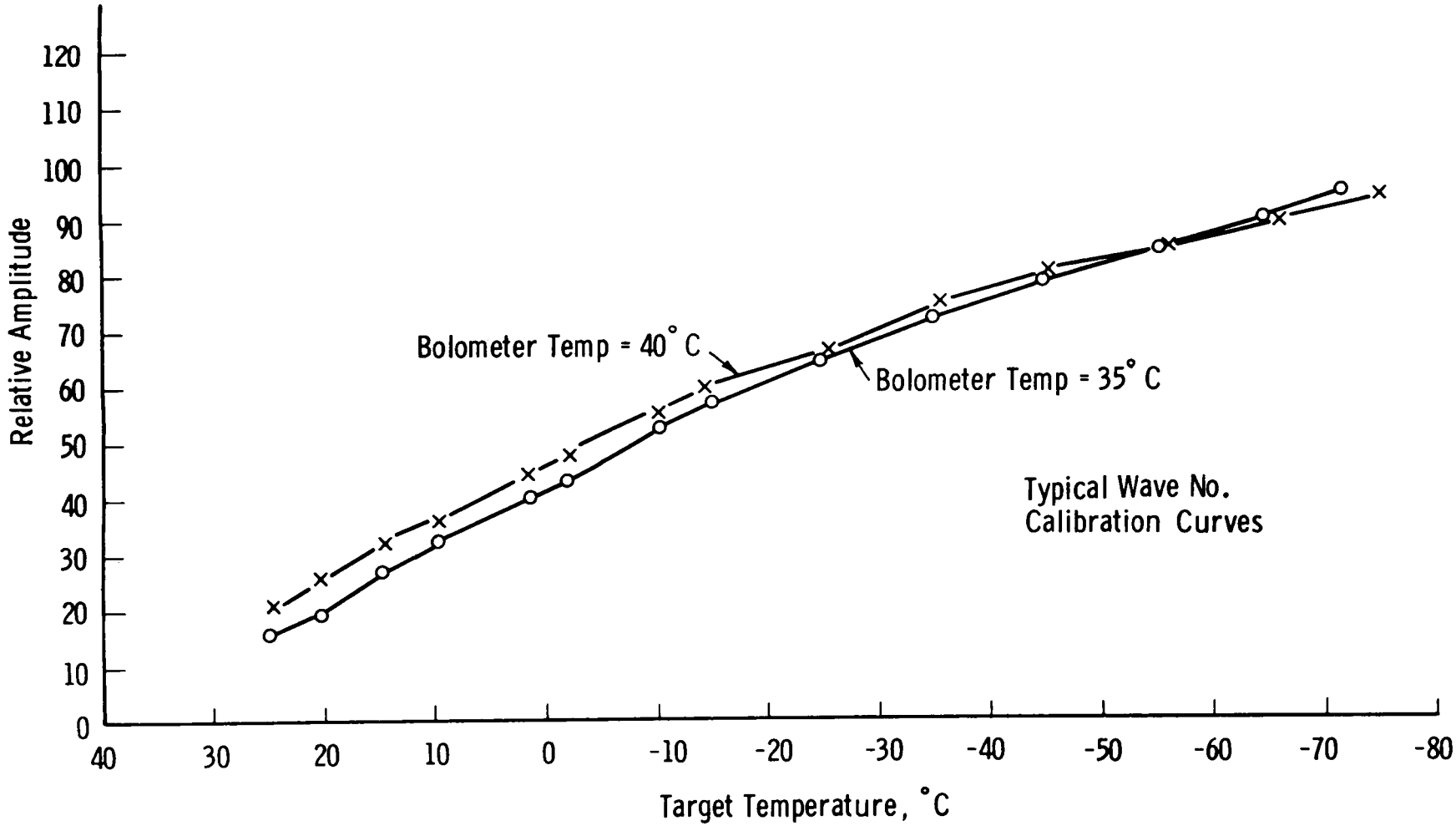

Fig. 25. Typical wave no. calibration curves.

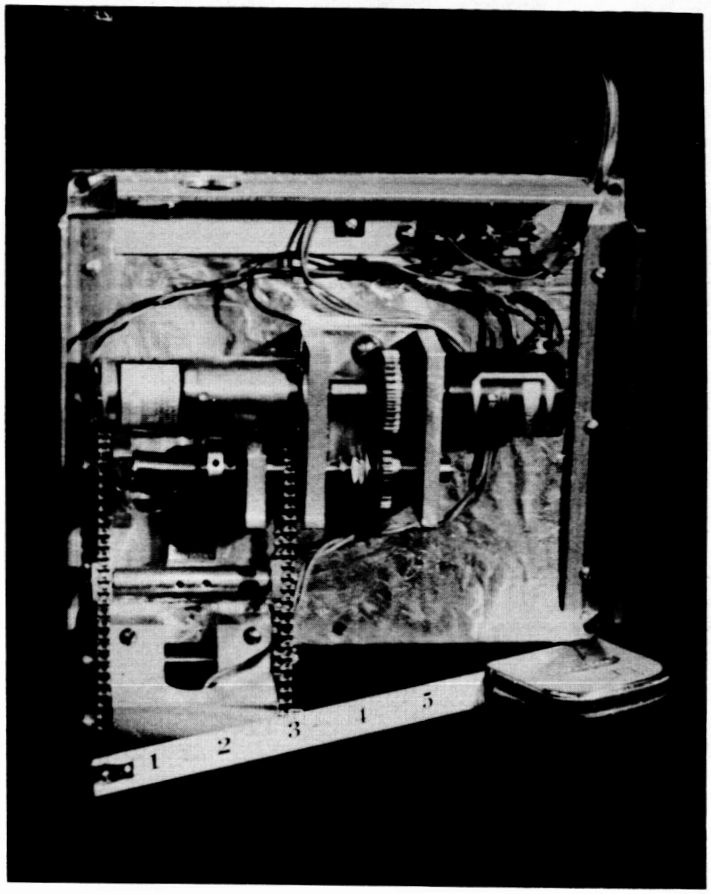

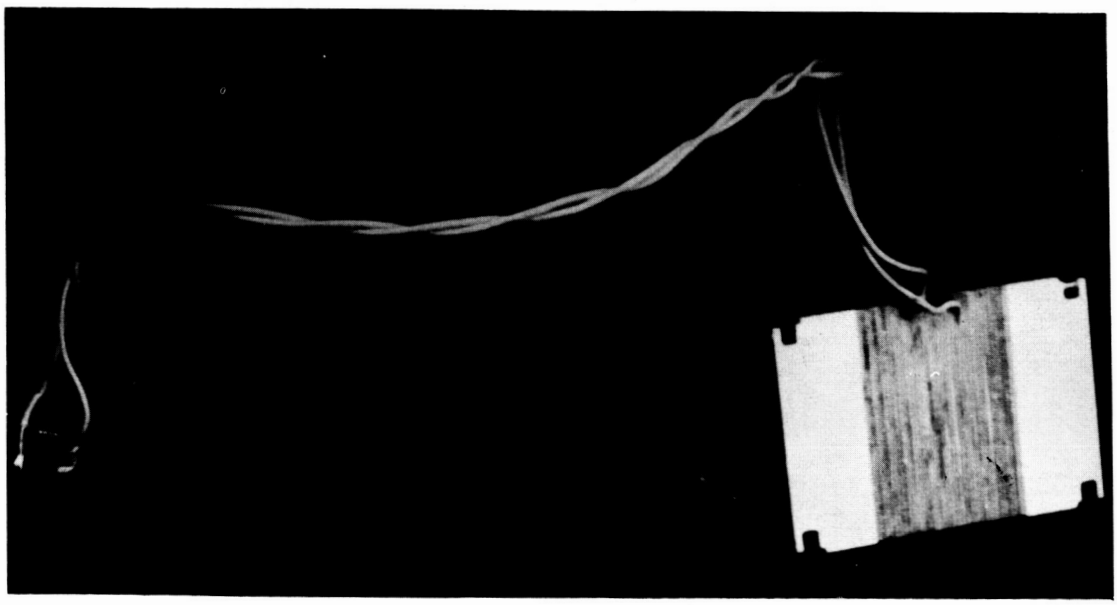

Fig. 26. Flight blackbody (photograph).

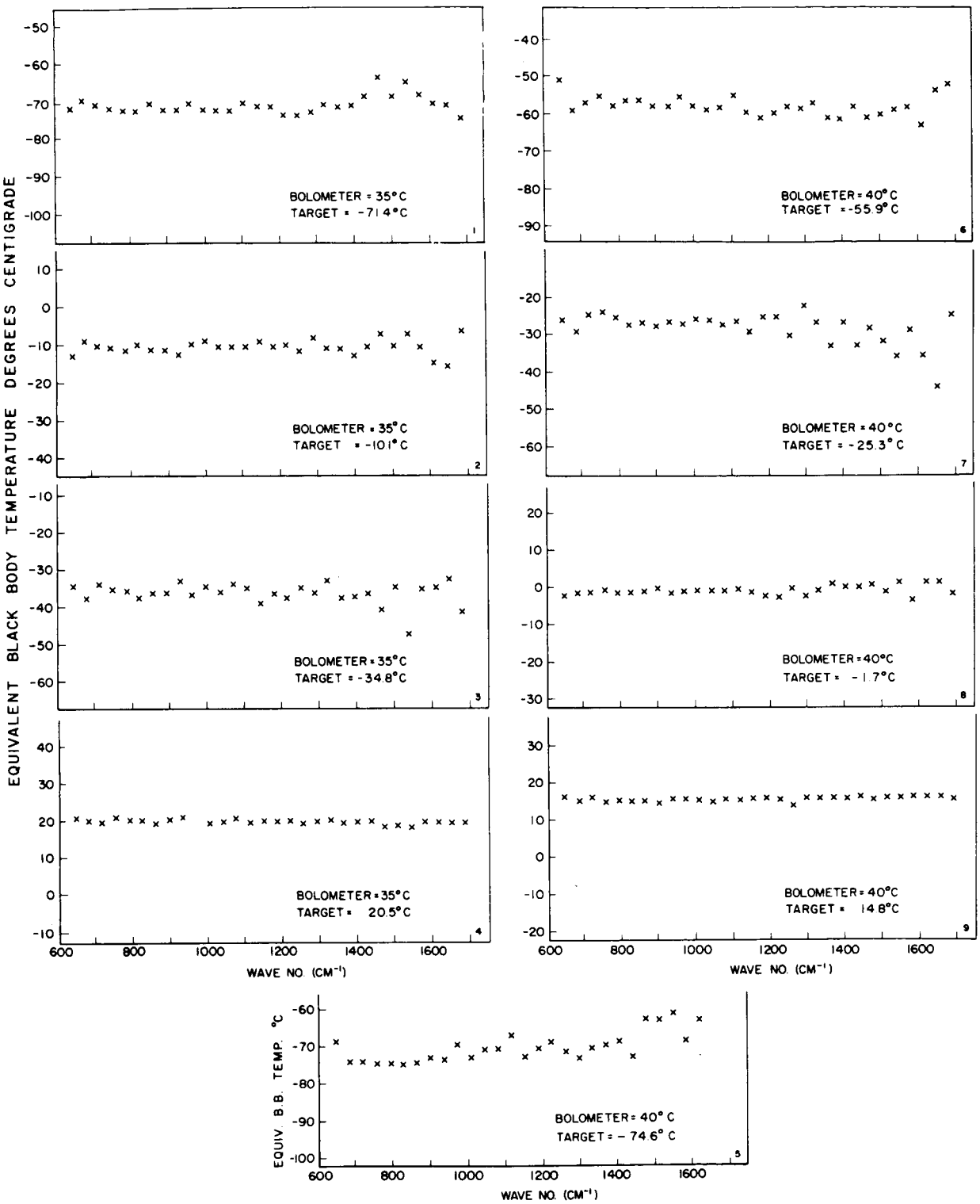

(a)

Fig. 27. Test data processed by the data reduction program: (a) Selected Data, (b) Typical Data.

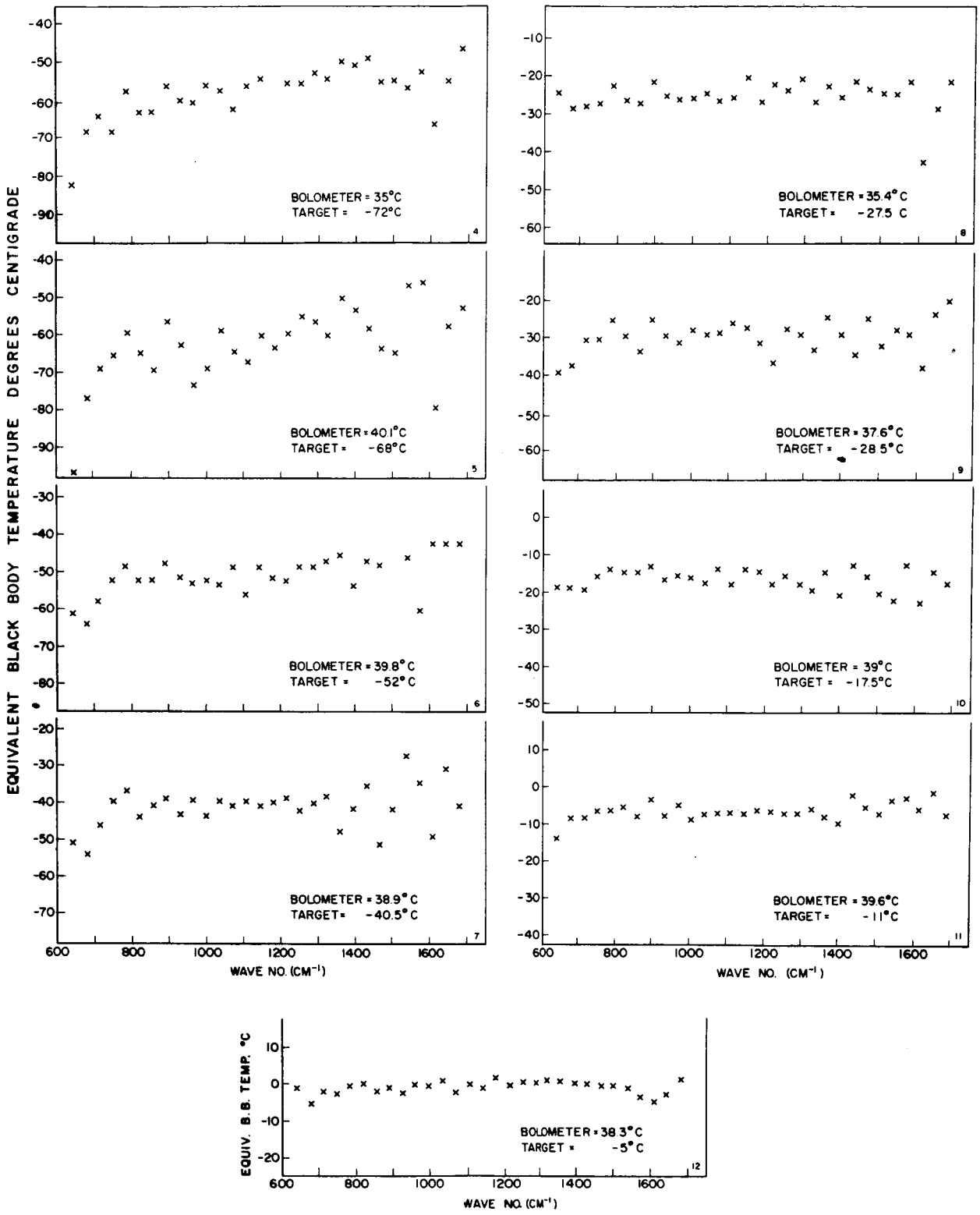

(b)

Fig. 27. (Concluded)